

# HEAT AND MASS TRANSFER IN HIGH TEMPERATURE SOLAR TECHNOLOGY FOR CEMENT PRODUCTION

The Presentation for the workshop for Department of Energy Science and Engineering Indian Institute of Technology Delhi Hauz Khas, New Delhi



# SOLAR RESEARCH AT THE GERMAN AEROSPACE CENTER

Part 1 of „Heat and mass transfer in high temperature solar technology for cement production“

Presentation by Prof. Dr.-Ing. Robert Pitz-Paal. Institutspraesentation komprimiert: Solar research at the German Aerospace Center. 2023



# German Aerospace Center Research Centre + Space Agency + Project Management Agency



AERONAUTICS



SPACE



ENERGY



TRAFFIC



SECURITY

Civil & Defence Security Research



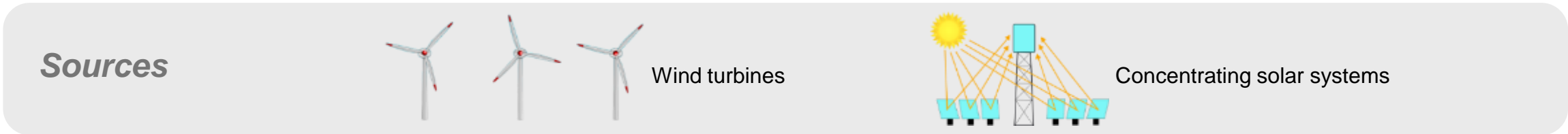
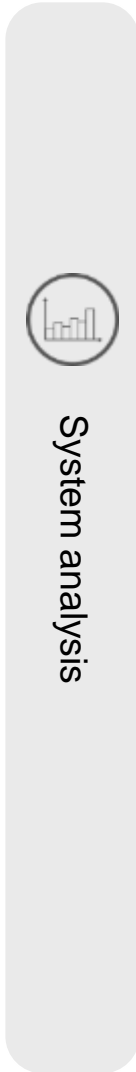
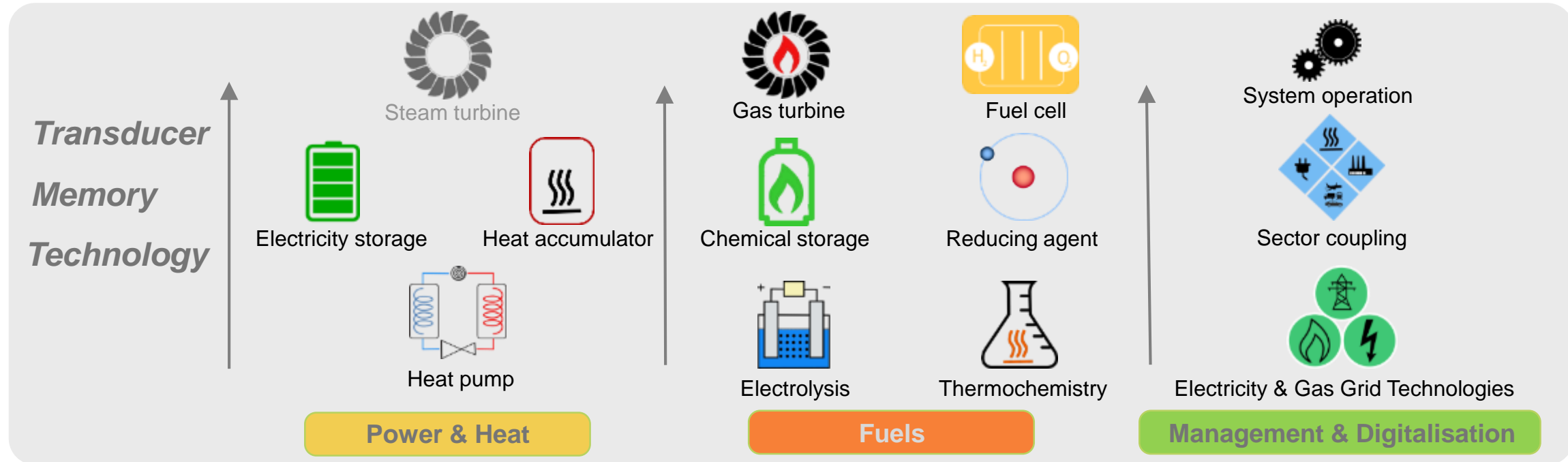
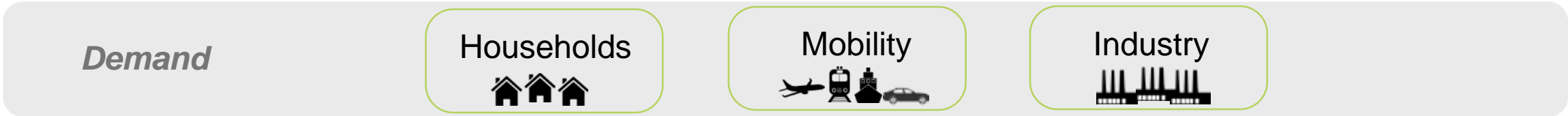
DIGITISATION

Quantum Technologies & Systems Modelling

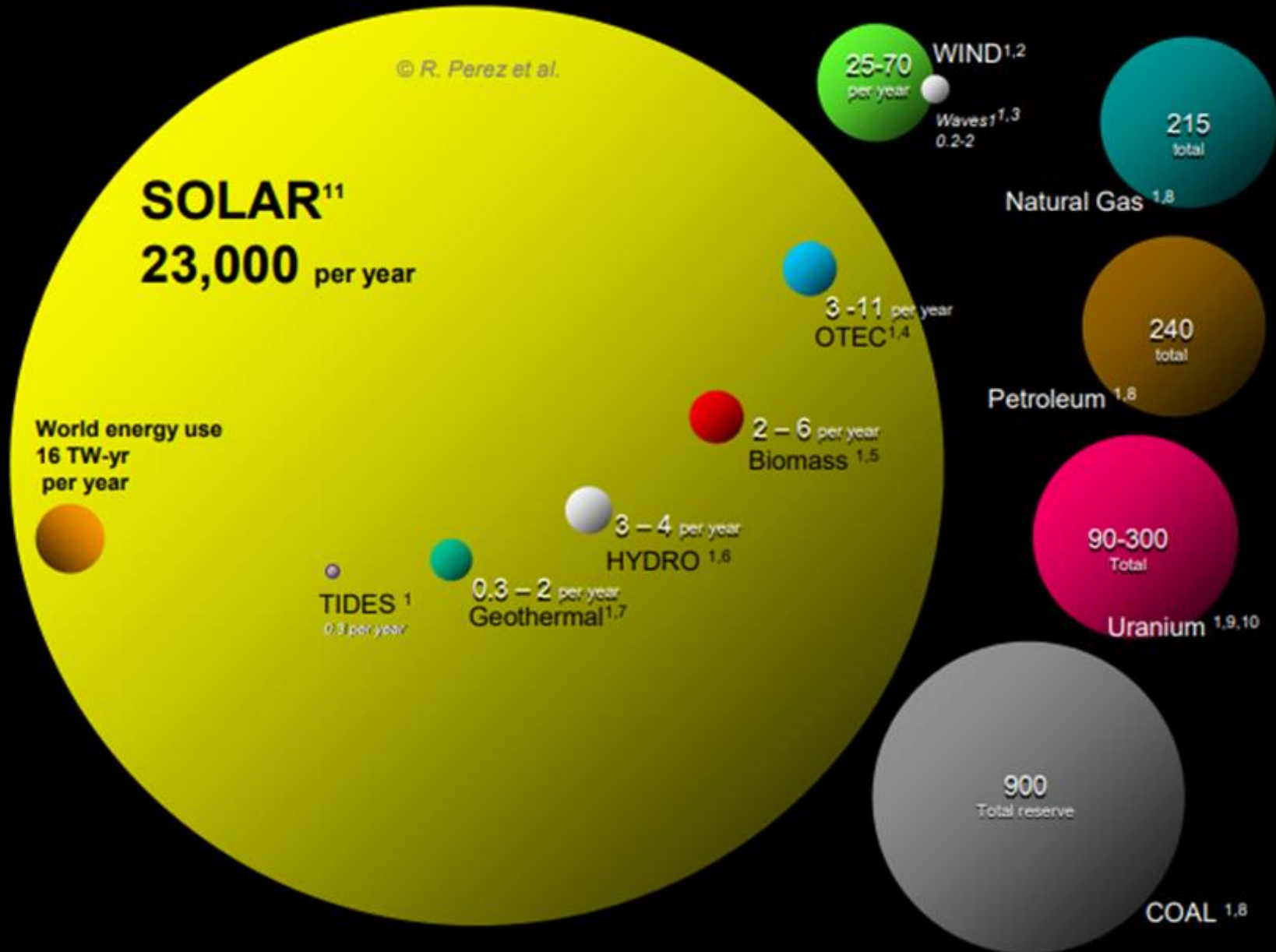




# DLR Energy Research: Controllable Sustainable Energy



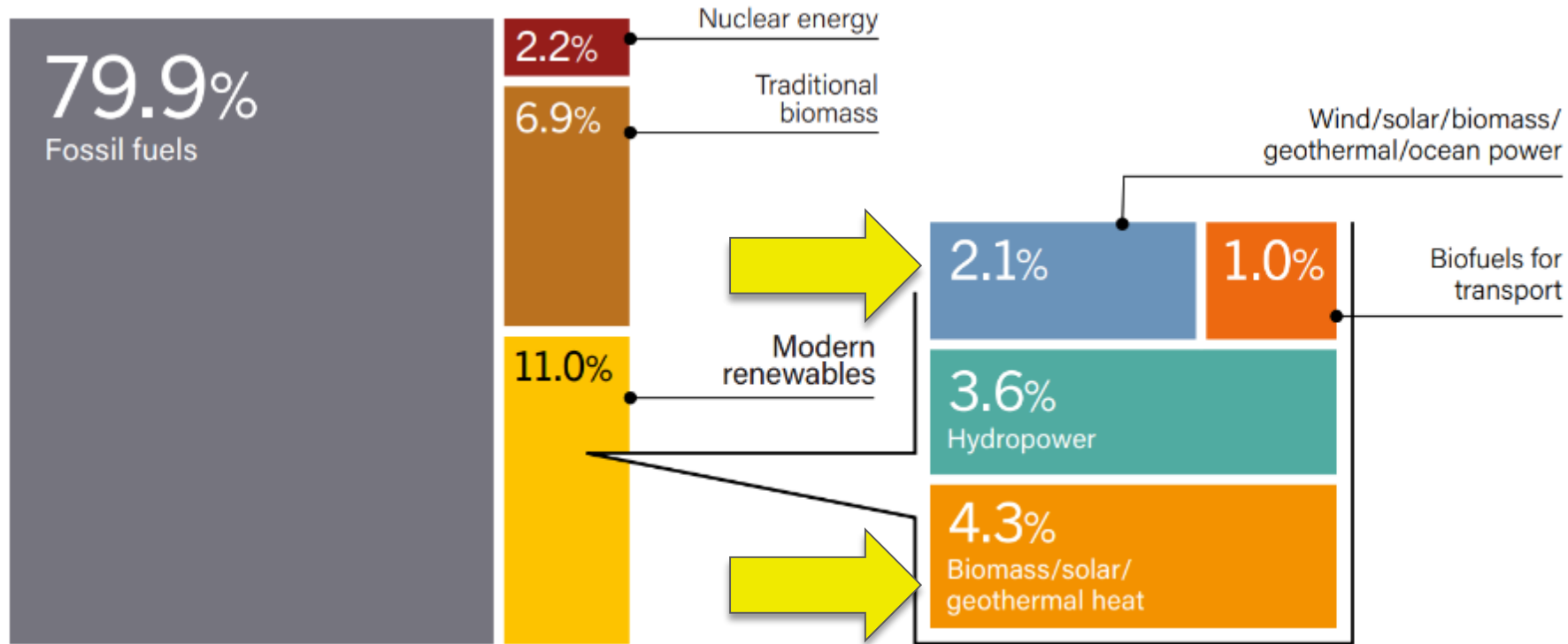
# The sun: energy for the future



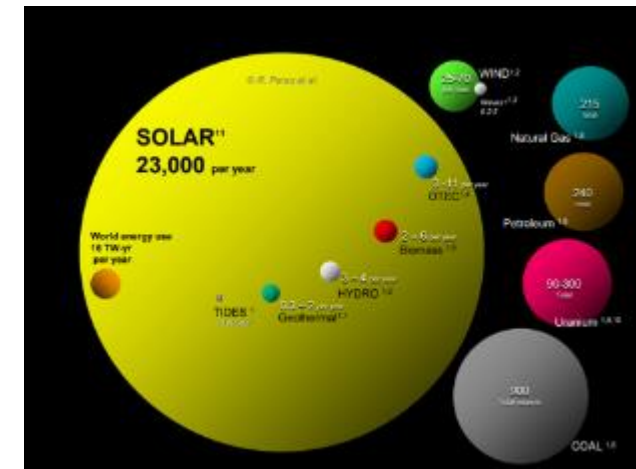
## Available solar energy:

- More than 90% of renewable energy resources
- Energy for 10,000 Earths

# Energy resources used worldwide



Source: REN21 (2020): Global Stature Report 2020 (figures from 2018).



# Institute of Solar Research



Concentrating solar technologies



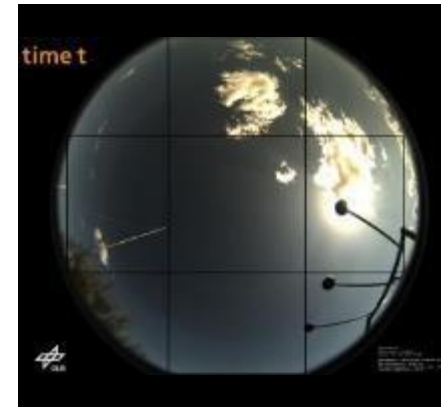
Quality assurance and operational optimisation for solar power plants and photovoltaic systems



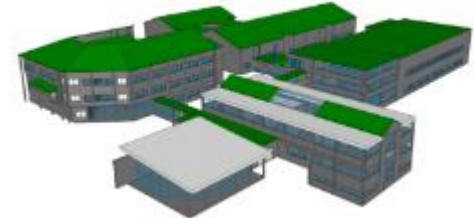
Agri Photovoltaics



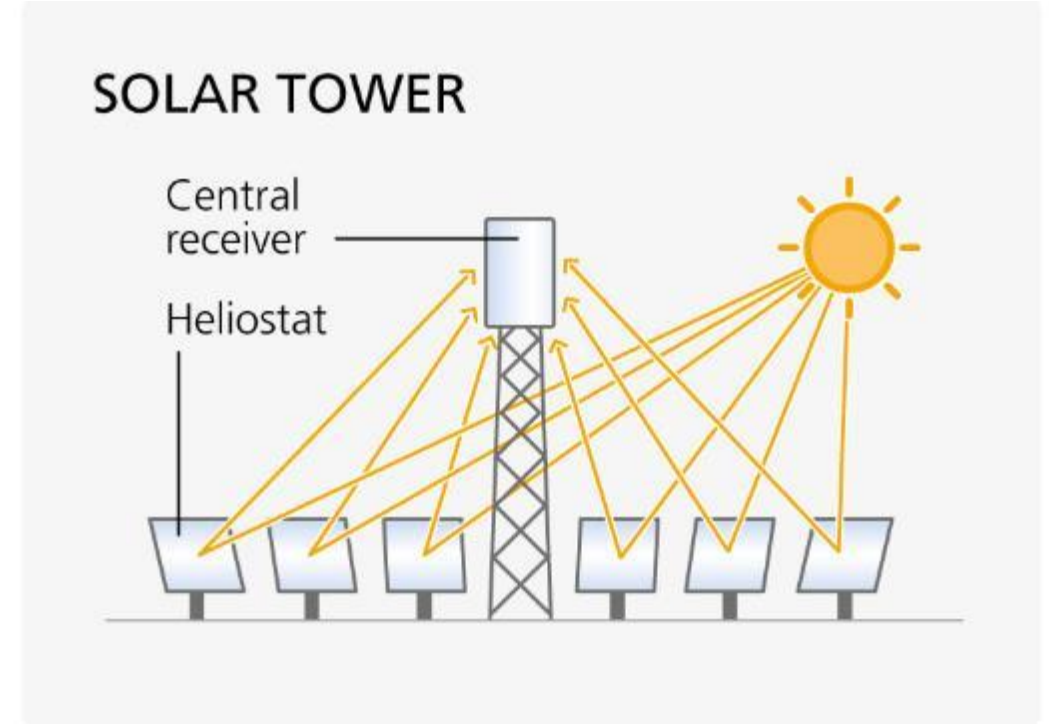
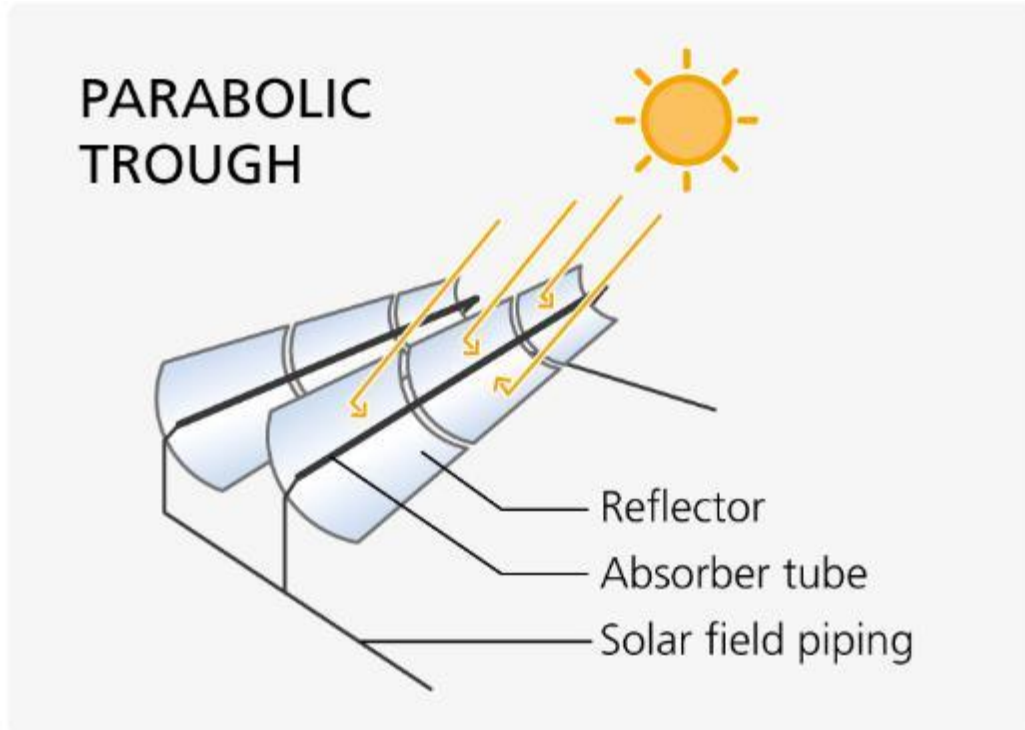
Solar energy meteorology



Heat transition: Energetic building assessment

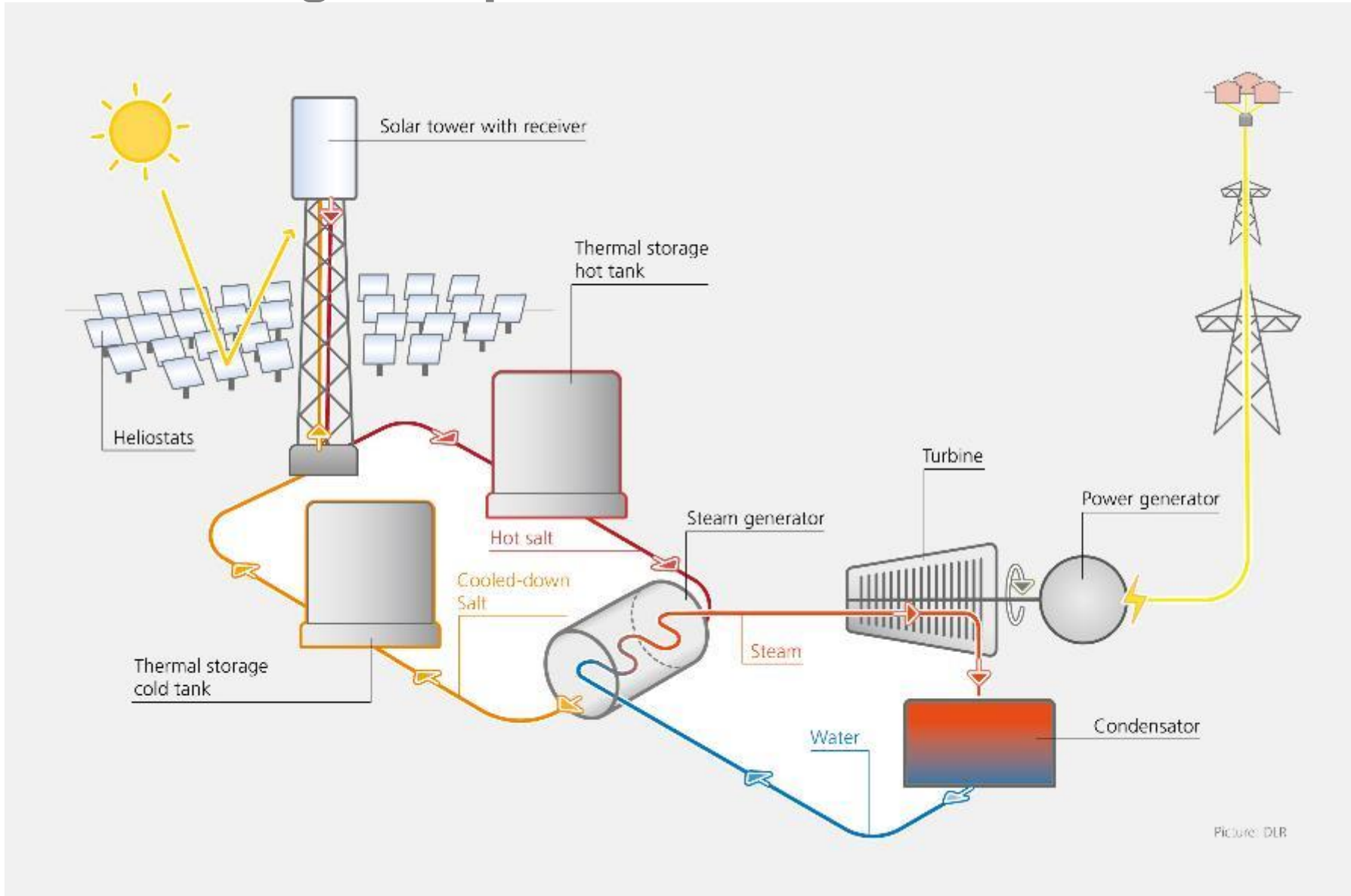


# In a nutshell: How does a solar thermal power plant work?

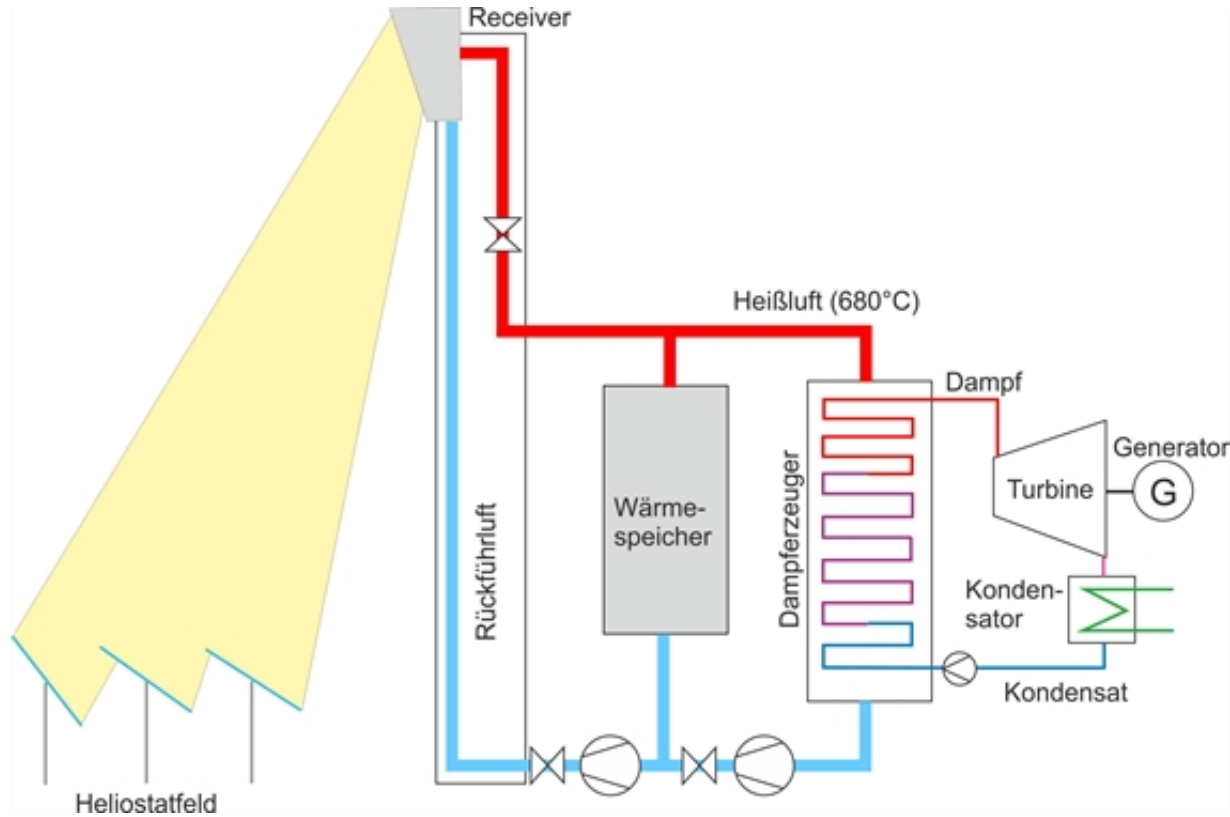




# In brief: from high temperatures to electric current



# Solar tower with air as a heat carrier



# The advantages of CSP technologies in a renewable energy system



- CO<sub>2</sub>-free
- Sustainable energy storage
- 24/7 Energy
- Adjustable
- Hybrid power plants with PV possible
- Can be used in district heating networks
- Can provide process heat for industrial plants
- Without rare resources

# Milestones of the Institute of Solar Research



02/2011

DLR founds  
**Institute of  
Solar  
Research**



06/2011

Takeover of the  
**Jülich Solar  
Tower**



03/2017

Inauguration  
of **Synlight** in  
Jülich



06/2020

Spin-off of the  
**Institute of  
Future Fuels**



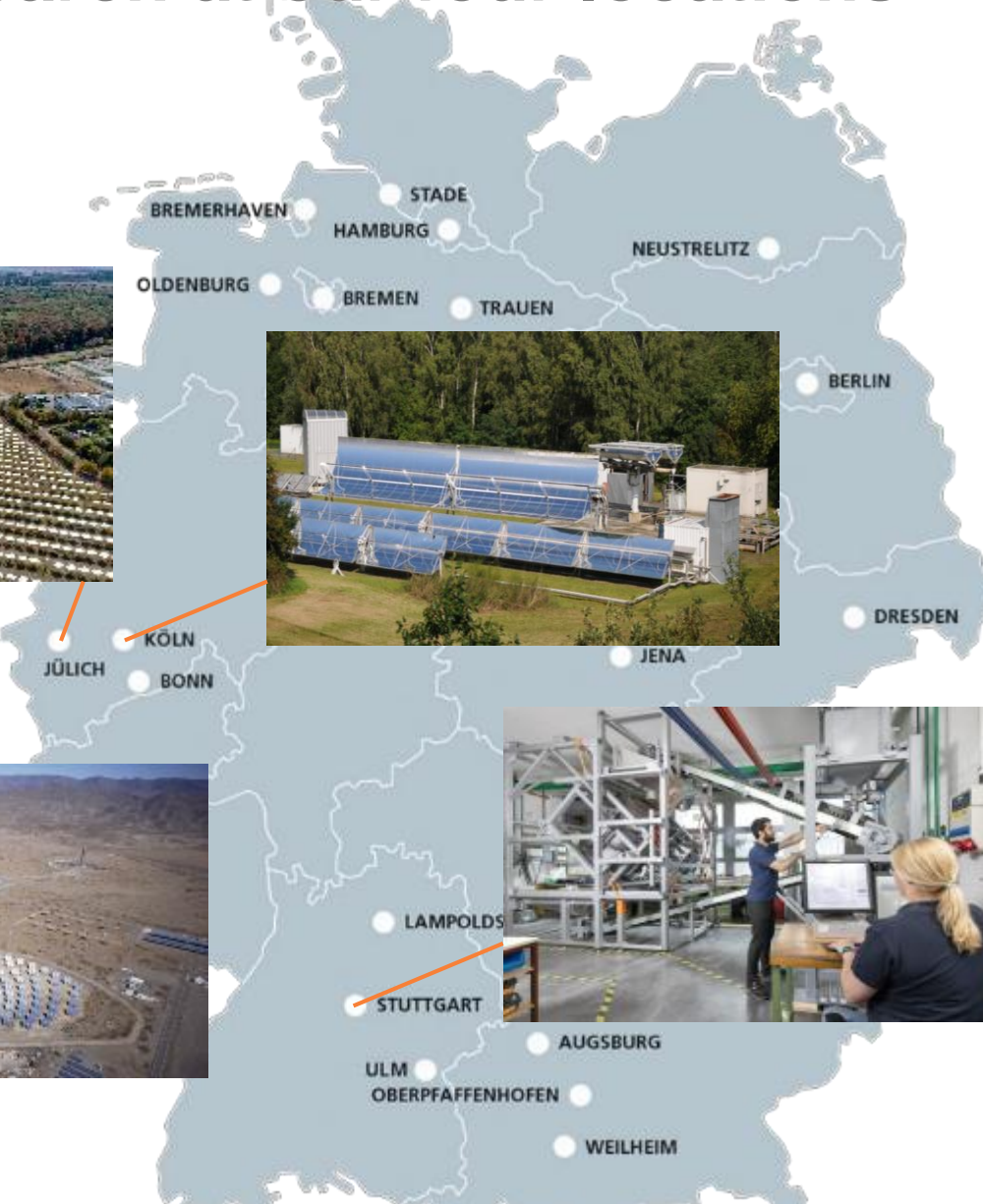
07/2020

Inauguration of  
the Jülich  
**Multifocus  
Solar Tower**

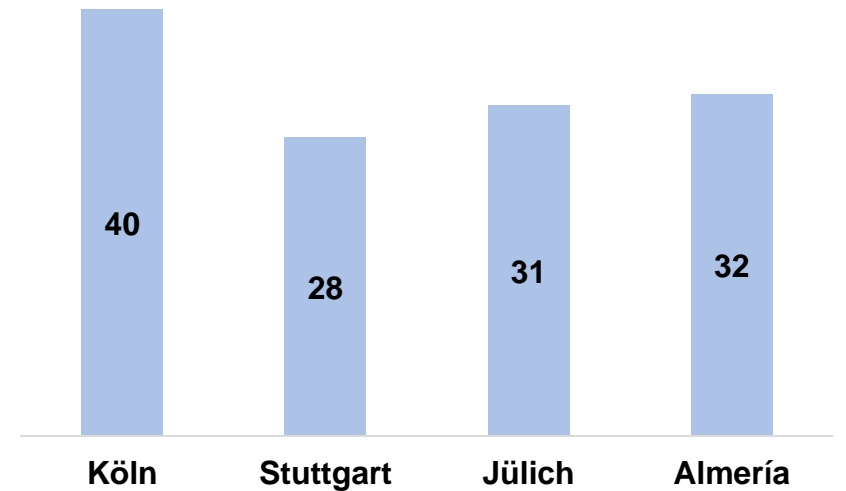




# Solar research at our four locations



● Almería (Spain)



Departments for the development and optimisation of solar thermal power plants

Technology development: efficient and economic use of solar energy for the production of electricity, heat and fuels

Solar high temperature technologies



Solar power plant technology



Qualification



Chairs in Aachen

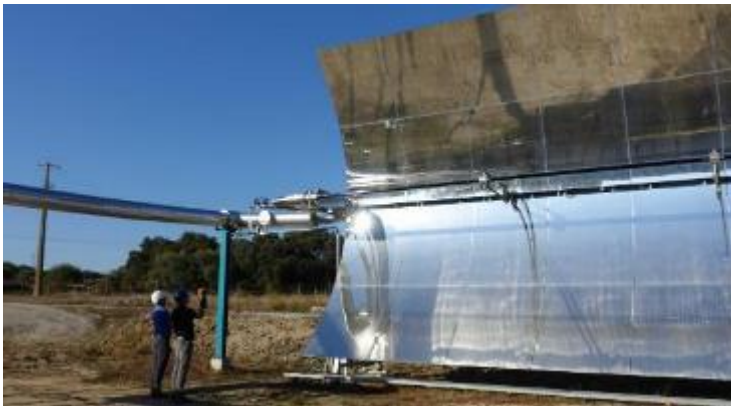


# Department Solar High Temperature Technologies



Head of Department: Dr.-Ing. Reiner Buck

**"Fluid Systems"**  
Dr.-Ing. Jana Stengler



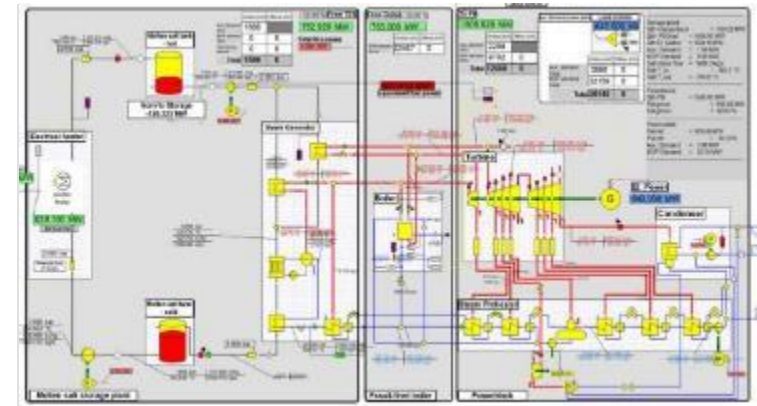
- Heat transfer in liquids and gases
- Operation of liquid salt plants
- Solar process heat

**"Particle systems"**  
Dr.-Ing. Luka Lackovic



- Heat transfer in particles
- Development of particle receivers and heat exchangers
- CFD/FEM/DEM modelling

**"System Modelling"**  
Dr.-Ing. Tobias Hirsch



- System modelling and design
- Techno-economic evaluation
- Operating behaviour and control of parabolic trough systems

■ 30 employees at the locations and plants in Stuttgart, Cologne and Évora (Portugal)

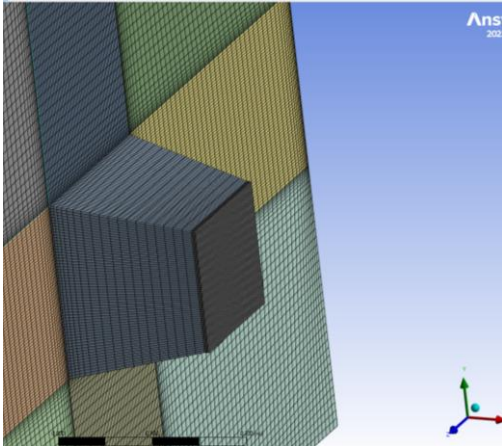


# Department Solar Power Plant Technology



Head of Department: Dr.-Ing. Kai Wieghardt

## "Simulation and Open Volumetric Receivers" Peter Schwarzbözl



- Controls for CSP and heliostat arrays
- Automation, dyn. simulation
- Flux density measurements

## "Jülich Solar Tower Power Plant" Felix Göhring



- Trial operation of the plants:
- Jülich experimental solar thermal power plant
- Multifocus Tower Jülich

## Employees at the Jülich site

Cheilytko Andrii, DLR, 26.11.2024 | New Delhy, Indian Institute of Technology Delhi



# Department Qualification



Head of Department: Dr.-Ing. Peter Heller

## "System qualification"

Dr.-Ing. Marc Röger



- Opt. qualification of solar fields
- Thermal characterisation of receiver systems

## "Solar Energy Meteorology"

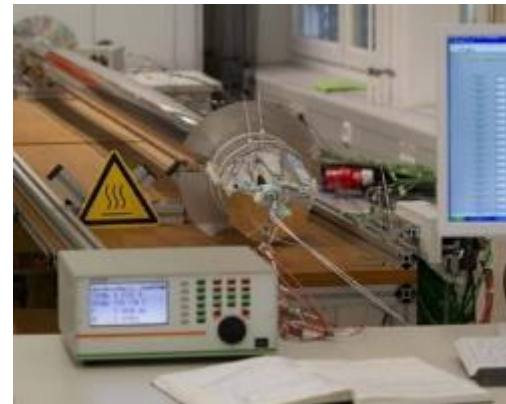
Dr. Stefan Wilbert



- Determination of meteorological parameters
- Analysis of the impact on CSP

## "Materials, Layers, Components"

Dr.-Ing. Florian Sutter



- Test methods and tests of components
- Durability of materials and components

## "Buildings and Quarters"

Dr. Jacob Estevam Schmiedt



- Energy analysis of buildings
- Basis for rehabilitation planning

40 employees at the sites in Cologne, Jülich, Oldenburg and Almería (Spain)



# PLATAFORMA SOLAR DE ALMERÍA

OWNER AND OPERATOR: CIEMAT



The background image shows a large industrial facility with several long, parallel solar collectors covered in blue glass panels. The facility is situated in a grassy area with a dense forest of green trees in the background. A yellow banner is overlaid at the bottom of the image.

# PROCESS HEAT TEST FACILITY





The image shows the Evora Molten Salt Platform, a large-scale solar thermal power plant. On the left, a long, curved array of heliostats (mirrors) is mounted on a metal frame, reflecting sunlight. To the right, a complex industrial structure with blue and yellow metal frameworks, pipes, and tanks is visible, representing the molten salt receiver and power cycle components. The entire facility is situated in an open, grassy field under a clear blue sky.

# EVORA MOLTEN SALT PLATFORM



# JÜLICH EXPERIMENTAL SOLAR THERMAL POWER PLANT



# Spin-offs of the Institute of Solar Research



2007



Optimising solar field performance and maximising system lifetime



2016



Heliostat design and control. Today Synhelion Germany



2017



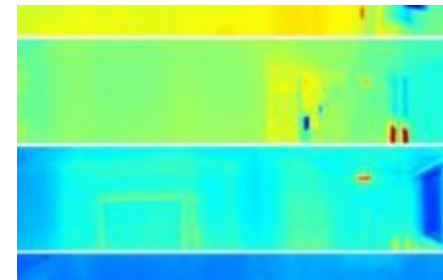
Particle receiver technology. Today part of Heliogen



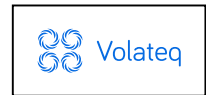
2019



3D capture and energy-efficient analysis of buildings



2020



Fully automatic condition monitoring of CSP and PV plants



- Development of alternative fuels

Technology development for the efficient and economic production of energy sources for a global, renewable energy economy

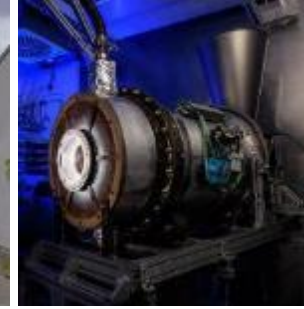
## Solar chemical processes



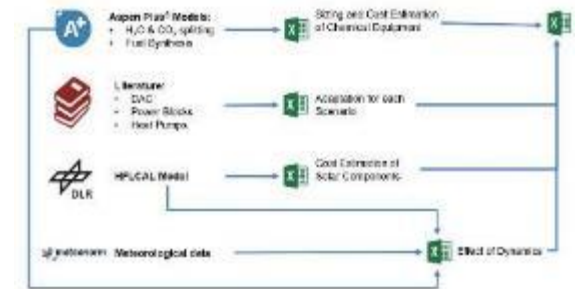
## Material and component design



## Demonstration



## Evaluation



# THE THEORY OF HEAT AND MASS TRANSFER PROCESSES IN SOLAR ABSORBER

Part 2 of «Heat and mass transfer in high temperature solar technology for cement production»





# The theory of heat and mass transfer processes in solar absorber



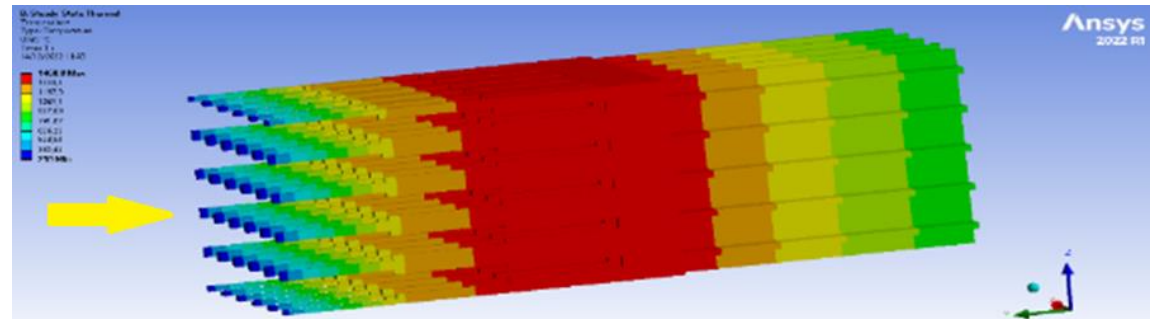
## Purpose

- Improve the quality and accuracy of existing calculations of heat and mass transfer processes in solar receivers.

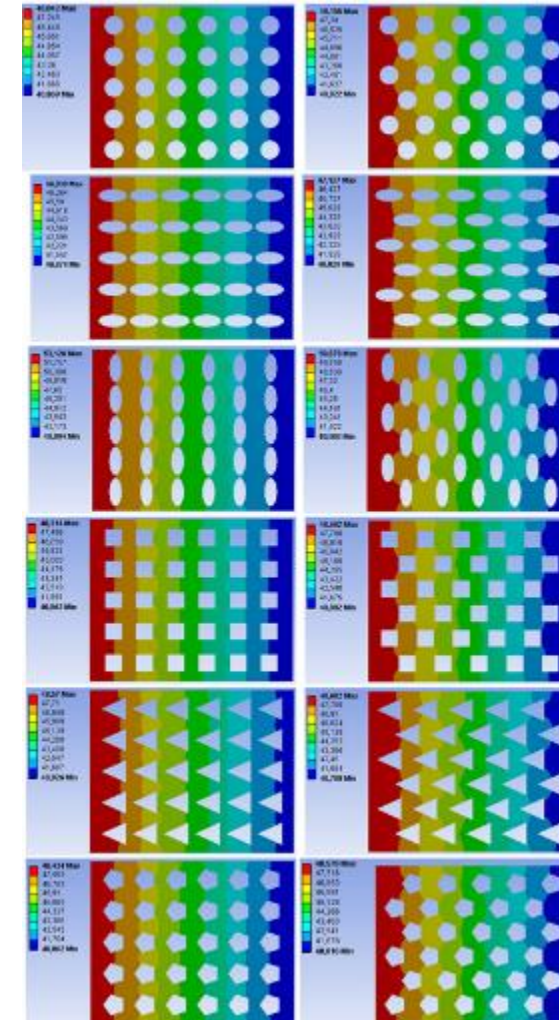
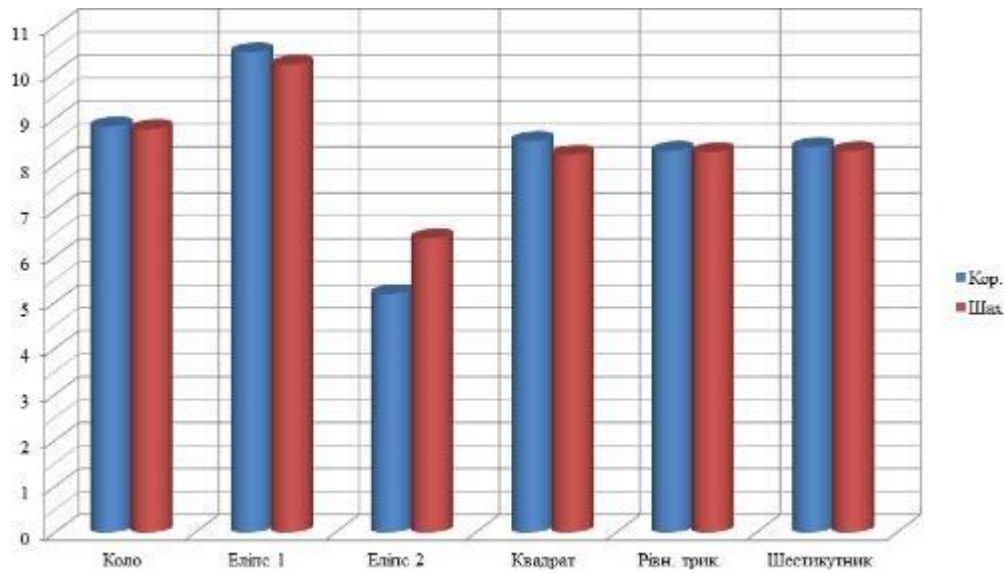
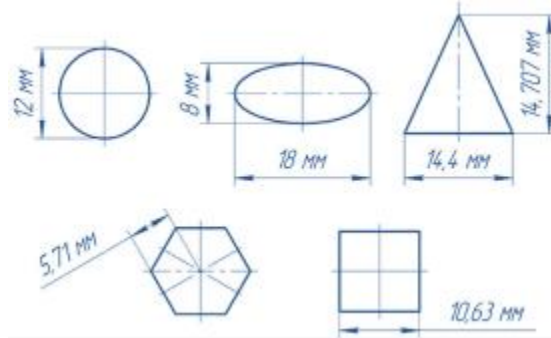
## Tasks

- AP 1 Basics
- AP 2 Modeling
- AP 3 Related technical tasks
- AP 4 Support to projects
- AP 5 Analysis of potential

$$\rho_s(c_p)_s \frac{\partial T_s}{\partial \tau} = \frac{\partial}{\partial x} \left( \lambda_s \frac{\partial T}{\partial x} \right) - \alpha A_v (T_s - T_f) + q_{source}$$
$$\rho_f(c_p)_f \left( \frac{\partial T_f}{\partial \tau} + u T_f \right) = \frac{\partial}{\partial x} \left( \lambda_f \frac{\partial T}{\partial x} \right) + \alpha A_v (T_s - T_f) + q_{source}$$

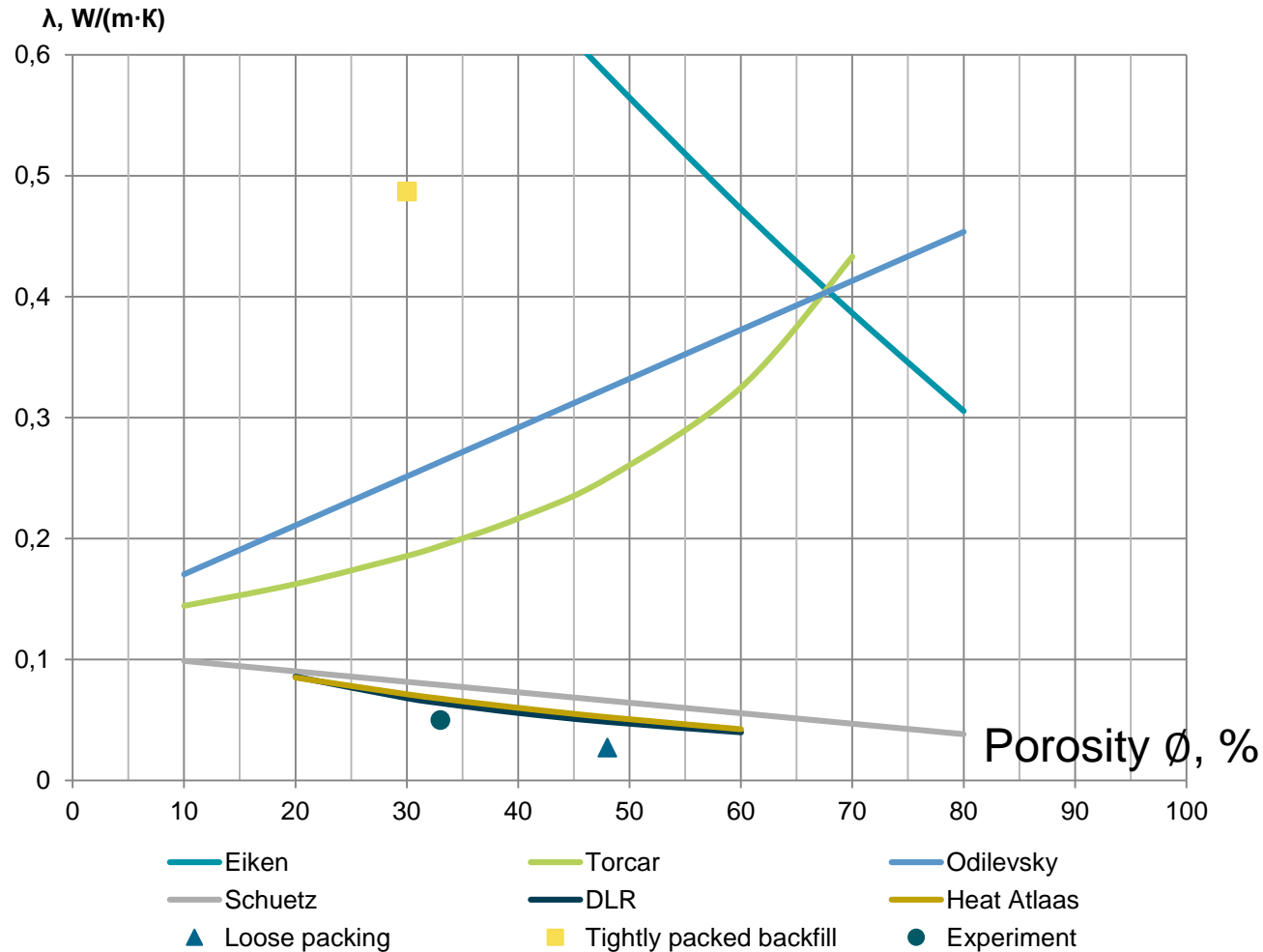


# Study of the influence of pore shape on the thermal conductivity coefficient of porous structures and thermal protection structures without taking into account convection inside the pores



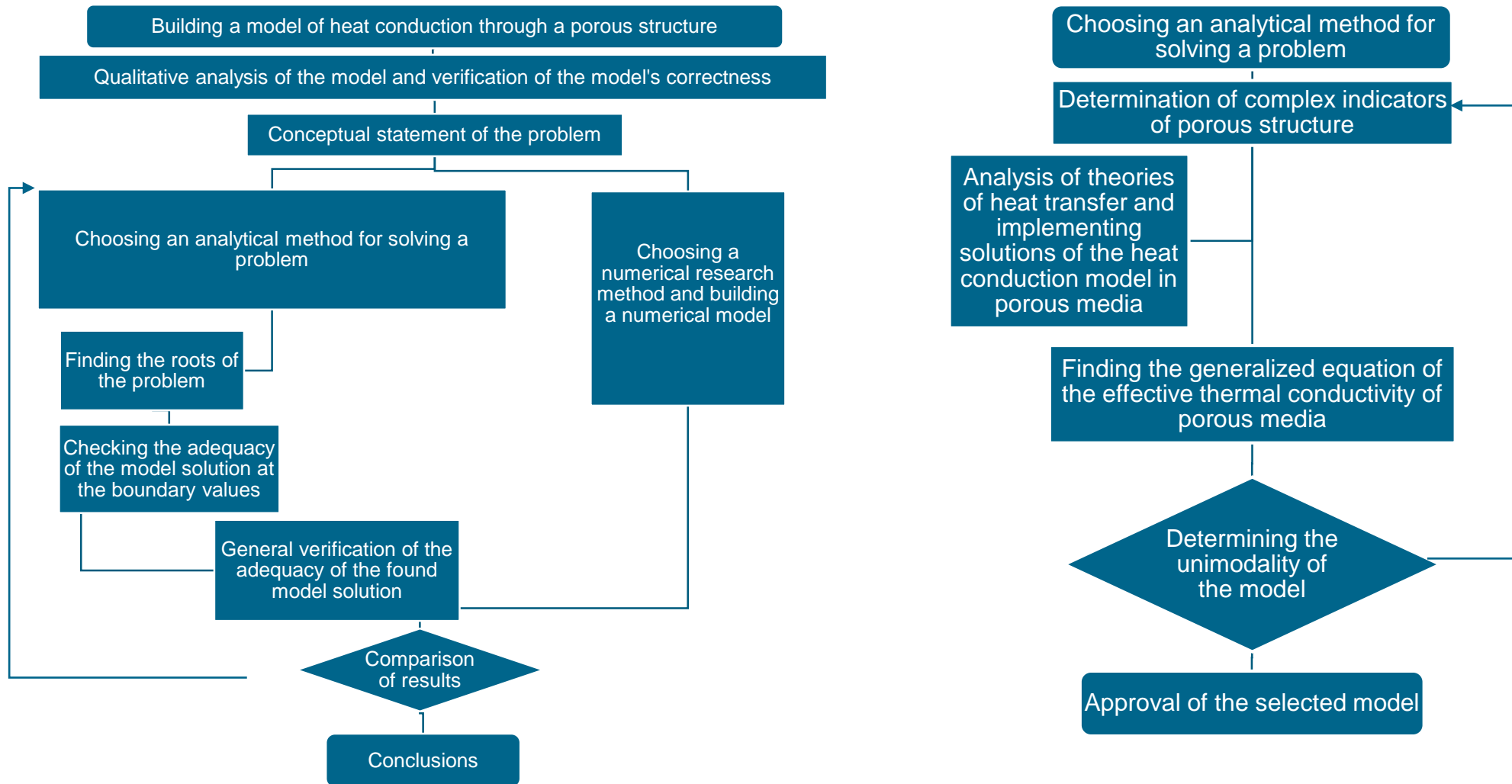
## Thermal conductivity coefficients of porous materials and products with different pore shapes

# Effect of porosity on the effective coefficient of thermal conductivity for backfills made of borosilicate glass





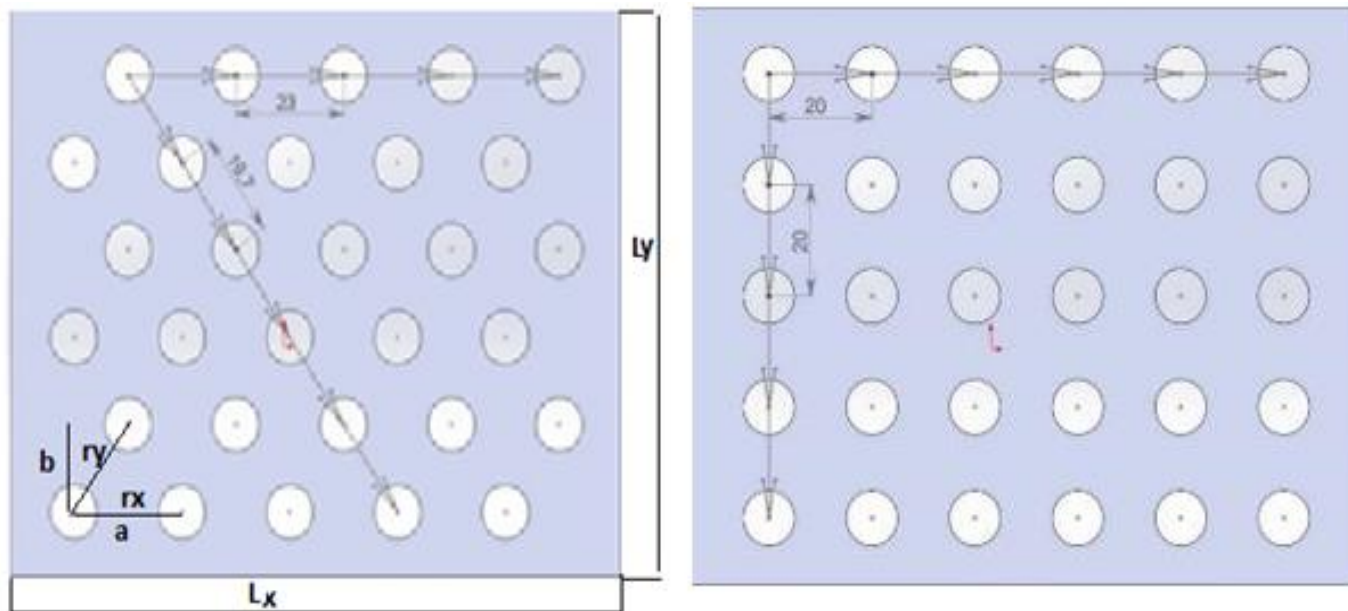
# Methodology for finding the equation of effective thermal conductivity



# The dislocation vector

The volume of a unit cell can be calculated from the constant lengths and angles of the lattice. If the sides of the cell are represented as vectors, the volume is equal to the scalar triple product of these vectors

$$V_{cell} = asb\sqrt{1 + 2\cos\alpha\cos\beta\cos\gamma - \cos^2\alpha - \cos^2\beta - \cos^2\gamma}$$



Locations with vectors on them  $k_y=1.182$  (left),  $k_y = 1$  (right)

$$(\bar{k}_y)_y = n_y \langle r_y \rangle / L_y$$

$$(\bar{k}_y)_x = n_x \langle r_x \rangle / L_x$$



# New equation



Equation DLR of the effective coefficient of thermal conductivity

$$\lambda_{eff,s} = \frac{\frac{\lambda_f \lambda_s}{\lambda_s \emptyset + \lambda_f (1 - \emptyset)}}{\frac{\lambda_s}{\lambda_f} \emptyset + 2\Psi + \frac{\lambda_f}{\lambda_s} (1 - \emptyset) + 1} \left[ \frac{\lambda_s}{\lambda_f} \emptyset + (1 - \emptyset) + \Psi \right] \left[ \emptyset + \frac{\lambda_f}{\lambda_s} (1 - \emptyset) + \Psi \right]$$

$\Psi$  - indicator of porous structure;

For different models of heat transfer, the solution of this model has different roots  $\Psi$ .

For open channel structure

$$\Psi = \frac{1}{k_y} (\emptyset - 1) \frac{(\lambda_s - \lambda_f)}{\lambda_s \lambda_f} [\lambda_f (\emptyset - 1) - \lambda_s (\emptyset)]$$

For porous mesh or catalyst, the following solution is recommended (this equation considers the uncertainty of  $k_y$ )

$$\Psi = (\emptyset - 1) \frac{1 - \frac{\lambda_f}{\lambda_s} + \sqrt{\left(1 - \frac{\lambda_f}{\lambda_s}\right)^2 + 4}}{2} + \emptyset \frac{1 - \frac{\lambda_s}{\lambda_f} + \sqrt{\left(1 - \frac{\lambda_s}{\lambda_f}\right)^2 + 4}}{2}$$

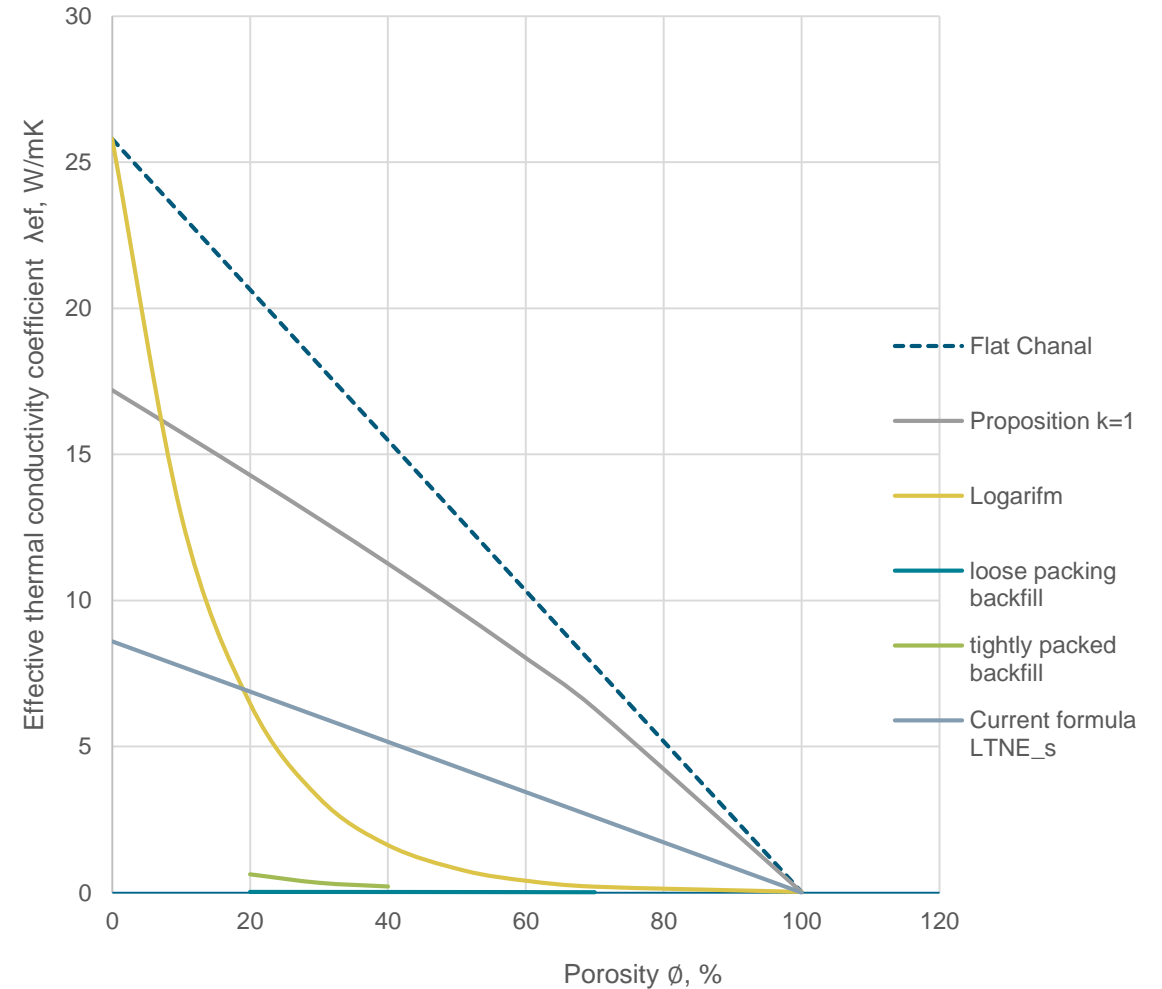
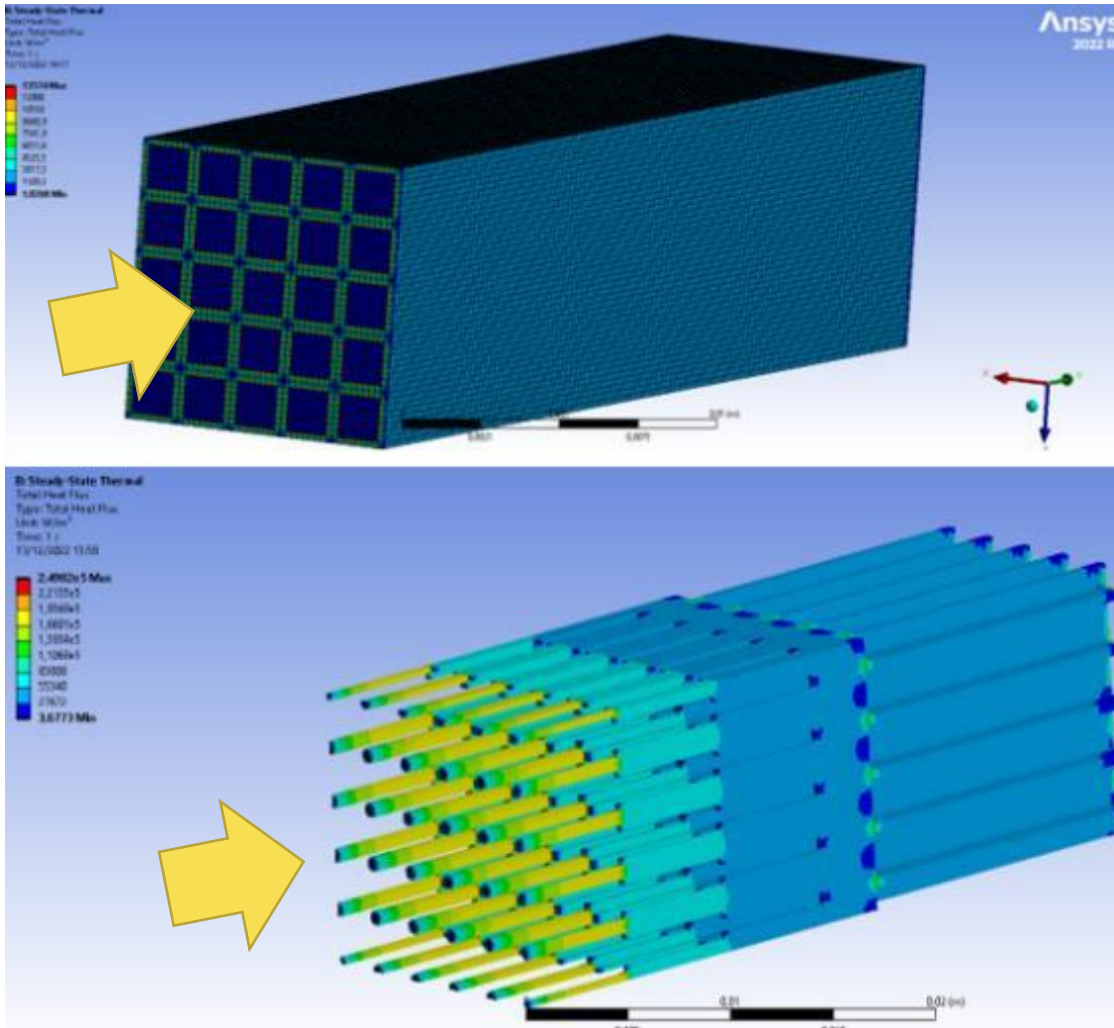
For fluid in the LTNE model

$$\Psi_f = \left( k_y \frac{1 - \frac{\lambda_f}{\lambda_s} + \sqrt{\left(1 - \frac{\lambda_f}{\lambda_s}\right)^2 + 4}}{2} \right)^{1-\emptyset} \times \left( k_y \frac{1 - \frac{\lambda_s}{\lambda_f} + \sqrt{\left(1 - \frac{\lambda_s}{\lambda_f}\right)^2 + 4}}{2} \right)^{\emptyset}$$

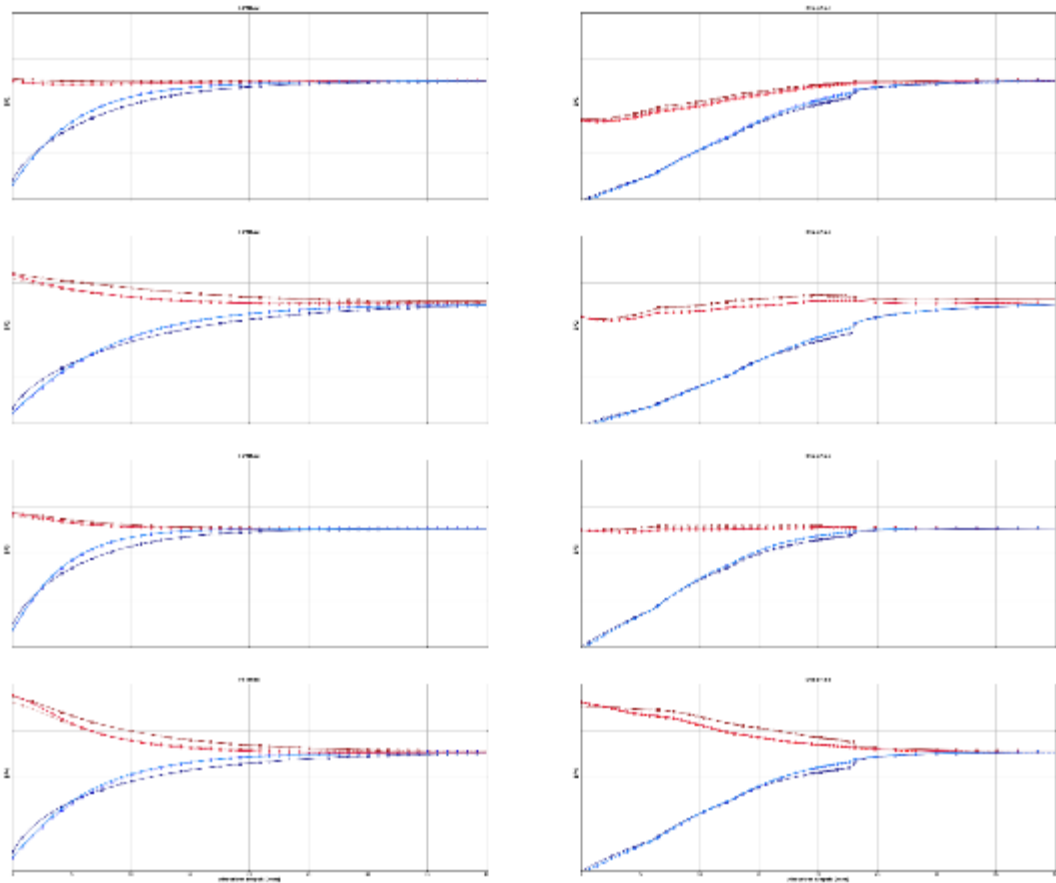
For porous open absorbers in the LTNE model

$$\Psi_s = \frac{1}{k_z} (\emptyset - 1) \frac{(\lambda_s - \lambda_f)}{\lambda_s \lambda_f} [\lambda_f (\emptyset - 1) - \lambda_s (\emptyset)]$$

# Comparison of different models of calculation of the effective coefficient of thermal conductivity



# Nu vs. Pe dependences for the StepRec type absorber with the capillary effect and effect from the thickness of the thermal layer and with considering the heat exchange of internal layers



*Depth dependence of air (blue) and solid (red) temperatures of HiTRec (left) and StepRec (right) absorbers for four different operating points (different angle and power of the irradiation energy)*



# Volumetric solid-fluid convective heat transfer coefficient

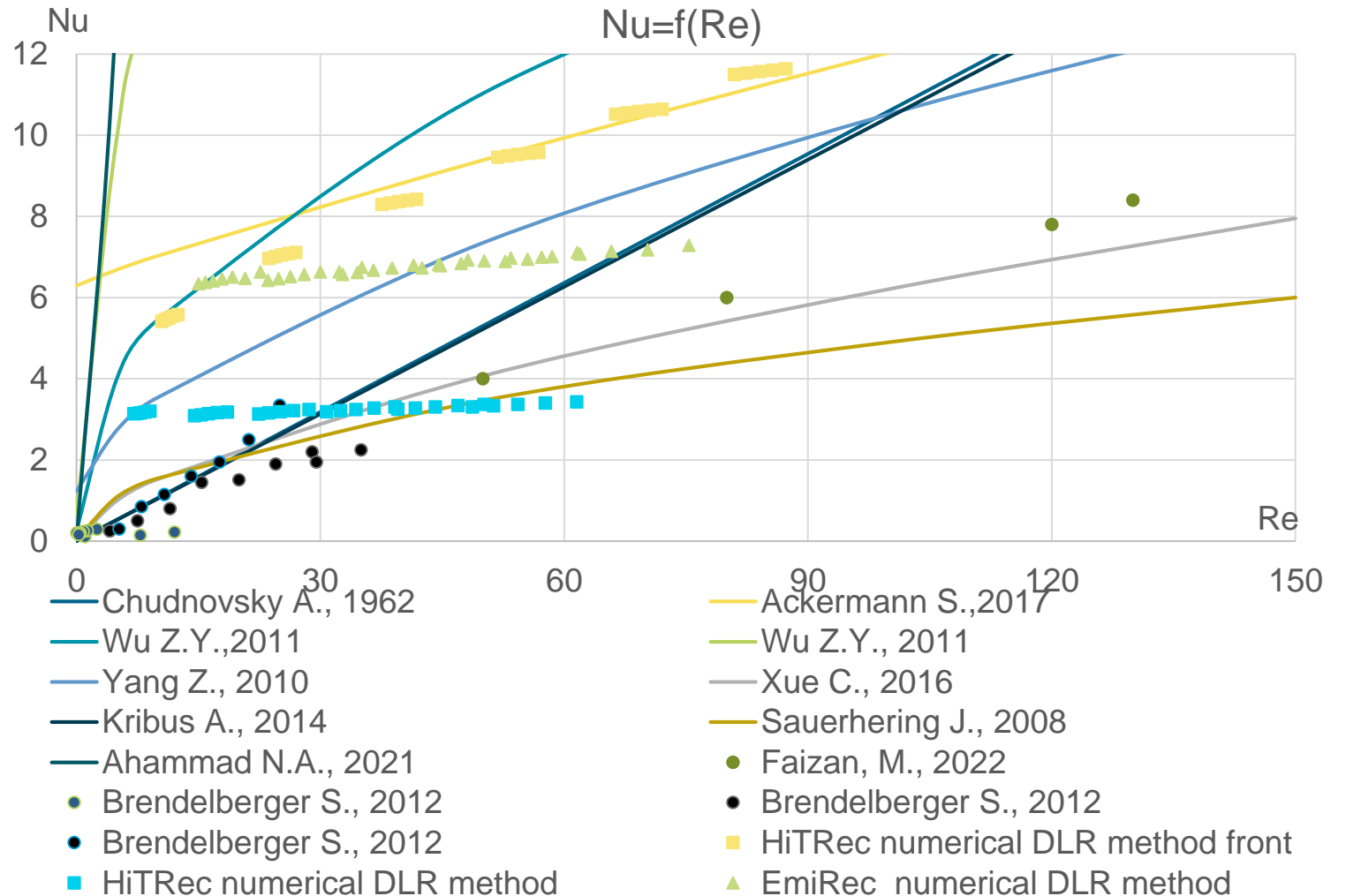


$$\frac{\partial}{\partial x} \left( \lambda_{s\_ef} \frac{\partial T}{\partial x} \right) - \alpha A_v (T_s - T_f) = 0$$

$$\frac{\partial}{\partial x} \left( \lambda_{f\_ef} \frac{\partial T}{\partial x} \right) + \alpha A_v (T_s - T_f) = 0$$

$$\alpha_v = \frac{Nu \cdot \lambda_f}{\langle d_{pore} \rangle}$$

$$Nu = \frac{Nu_0}{\tanh\left(2.43 Pr^{\frac{1}{6}} X^{\frac{1}{6}}\right)}$$



# How to determine the heat transfer coefficient?



The heat flux can be determined by the temperature gradient in the body or by the power of the electric heater. The wall temperature can be measured. The temperature of the liquid at a distance from the wall is a conditional value

Liquid temperature - average mass temperature in the channel

$$\bar{T} = \frac{\int \rho C_p w T dS}{\int \rho C_p w dS}$$

$$Nu = c Re^n Pr_f^m \left( \frac{Pr_f}{Pr_s} \right)^{0.25}$$

$$c = f(\Phi), \quad n = f(d_e, \bar{u}_b), \quad m = f(d_e)$$

$$\ln Nu = f(\Phi) + f(d_e, \bar{u}_b) \ln Re + f(d_e) \ln Pr_f + 0,25 \ln \left( \frac{Pr_f}{Pr_s} \right)$$

$$\left( \frac{Pr_f}{Pr_s} \right)^{0.25}$$

Mikheev amendment

**The average heat transfer coefficient on any surface F:**

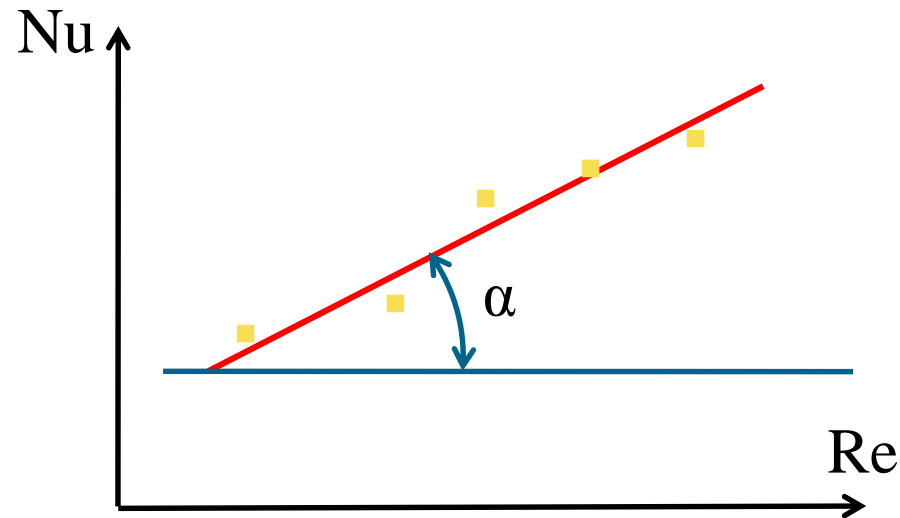
$$\bar{\alpha} = \frac{\bar{q}}{\Delta T} = \frac{\int_F q dF}{\int_F (T_{\text{жс}} - T_{cm}) dF}$$

Example of experimental data processing: at forced convection usually



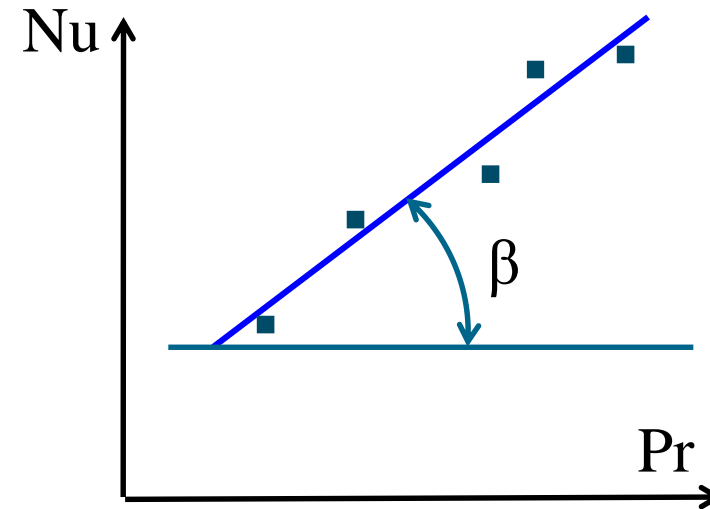
$$\text{Nu} = C \text{Re}^n \text{Pr}^m$$

$$\ln \text{Nu} = n \ln \text{Re} + m \ln \text{Pr} + C_1$$



Pr = const

$$n = \text{tg} \alpha$$

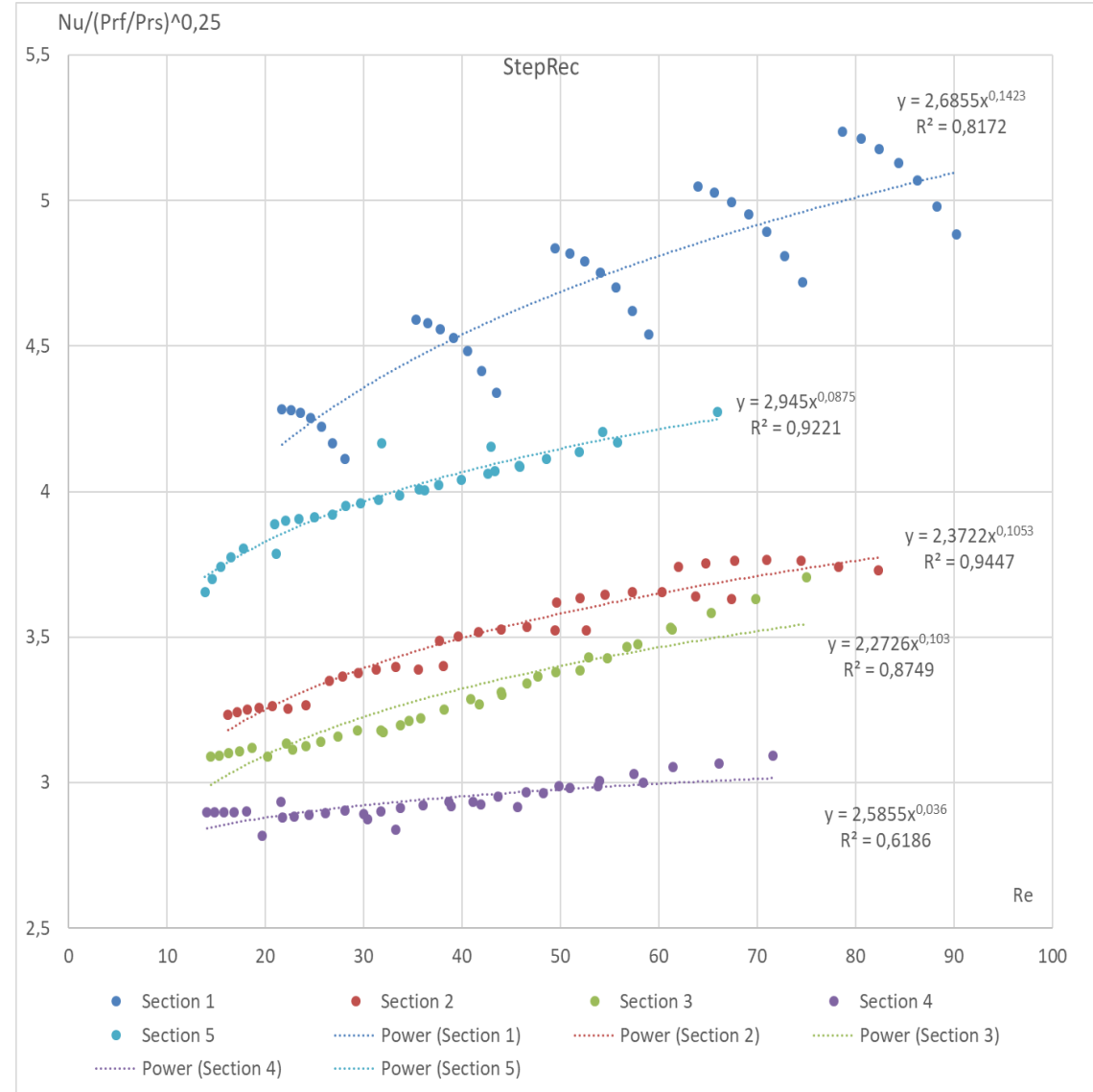
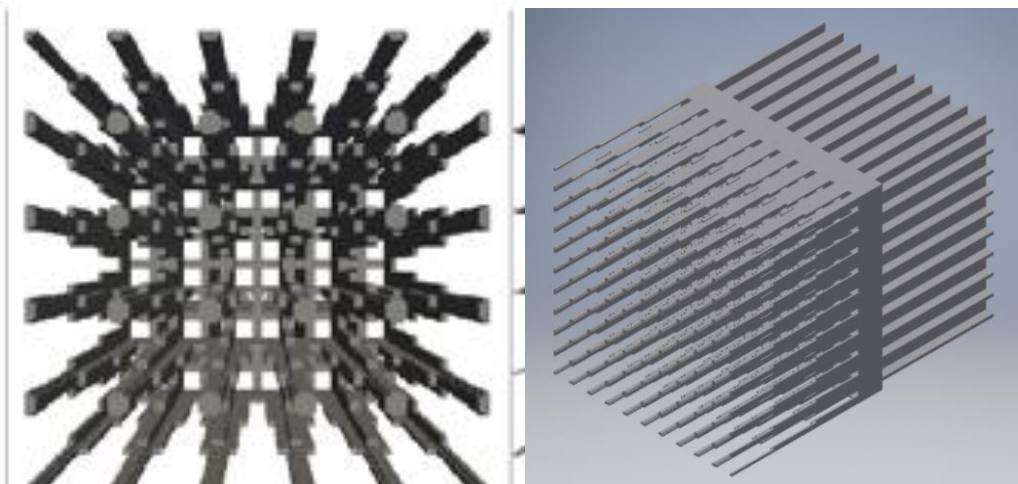
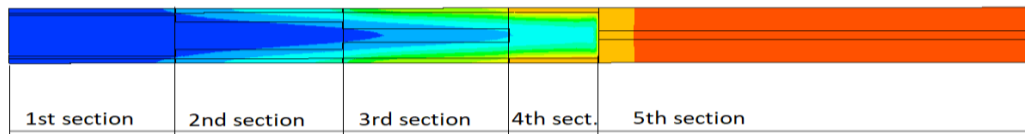
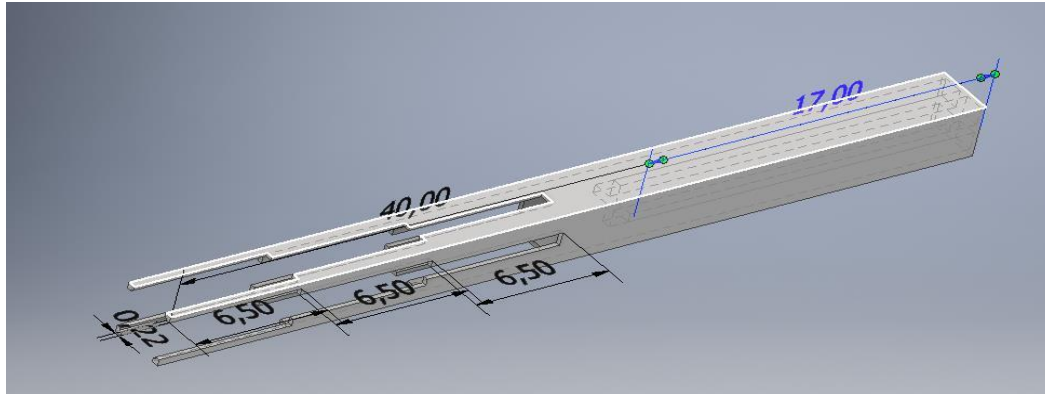


Re = const

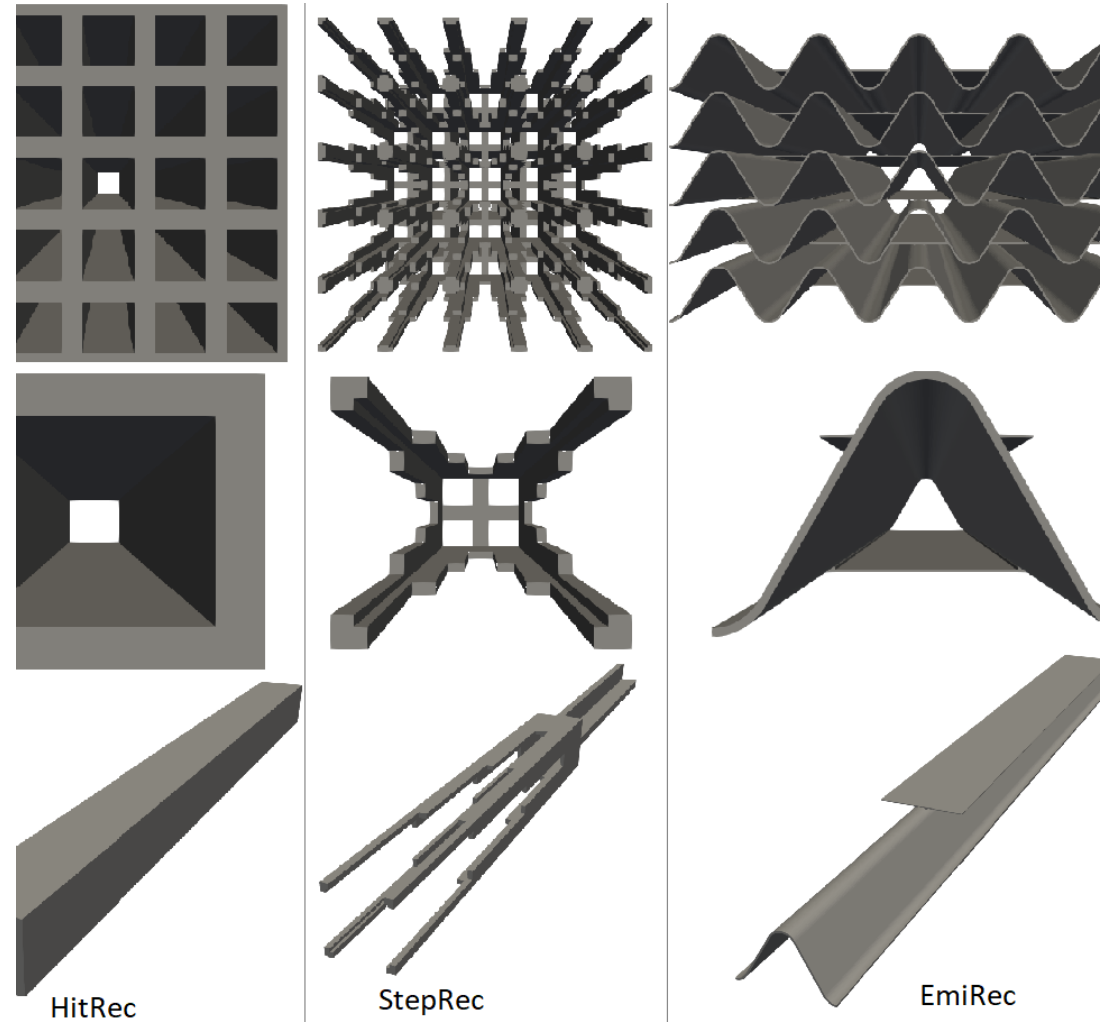
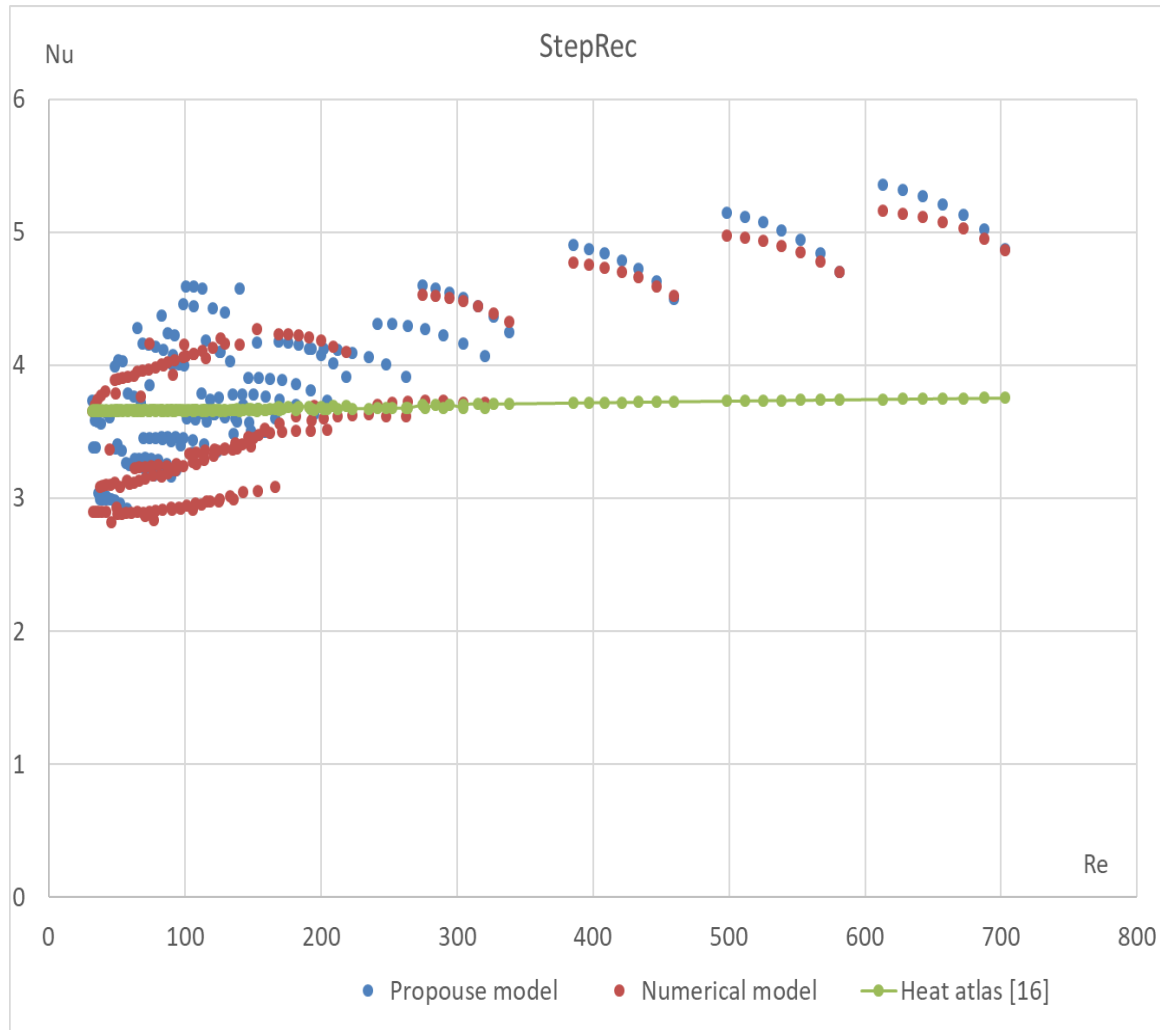
$$C = \frac{\text{Nu}}{\text{Re}^n \text{Pr}^m}$$



# Probleme



# Receiver's absorber



# Analytical Determination of Nusselt Numbers for Convective Heat Transfer Coefficients in Channel Macroporous Absorbers

$$Nu = c \cdot K^{stability} \cdot \text{Exp}\left(-0,5 \frac{T_{in}}{T_w}\right) \cdot \frac{d_e}{l_t} \cdot Re^n \cdot Pr_f^{0,33} \cdot \left(\frac{Pr_f}{Pr_s}\right)^{0,25},$$

$$c = c_1 \cdot \exp\left(c_2 \cdot \tan\left(\frac{1 - \phi}{\phi}\right)\right),$$

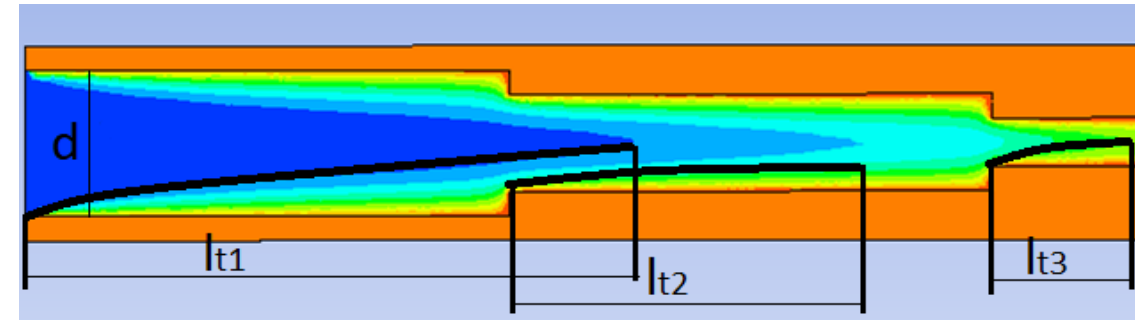
$$K^{stability} = \begin{cases} 1 & \text{if } l_t^{previous} < L^{previous} \\ 1 - 0,1 \frac{l_t^{previous} - L^{previous}}{L} & \\ 0,9 & \text{if } l_t^{previous} > L^{previous} \end{cases},$$

$$n = 0,015 \ln\left(\frac{d_e}{L}\right) + c_3 \left(\frac{c}{\phi} \xi_{Shape}\right)^{c_4},$$

$$\xi_{Shape} \approx \frac{d_e}{d_e^{previous}} + 1 + \frac{d_e}{d_e^{next}}.$$

$$l_T = k_T \cdot Re \cdot d \cdot Pr_f$$

$$k_T = 0,07$$



where  $\xi_{Shape}$  - coefficient changes shape of channel;

for first section  $\xi_{Shape} = \phi + 1 + \frac{d_e}{d_e^{next}}$  ;

for last section  $\xi_{Shape} = \frac{d_e}{d_e^{previous}} + 1 - \phi$  ;

$L$  – length of the channel;

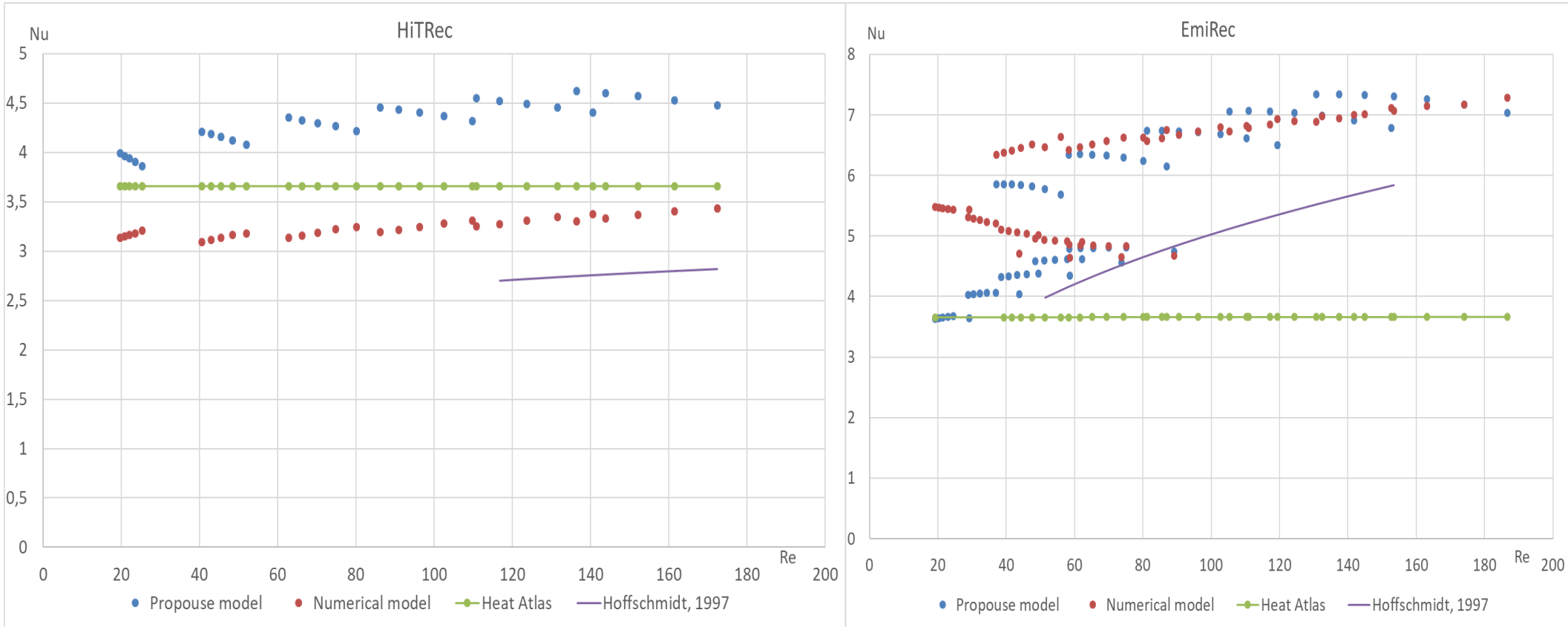
$l_t$  – length of the thermal boundary layer

$d_e$  – hydraulic diameter.

$c_1 = 0,1$ ;  $c_2 = 0,525$ ;  $c_3 = 1,1$ ;  $c_4 = -0,09$  are structural constants.



# Validation of the Nu number of the dependence on Re for all sections of absorbers with 30 different modes



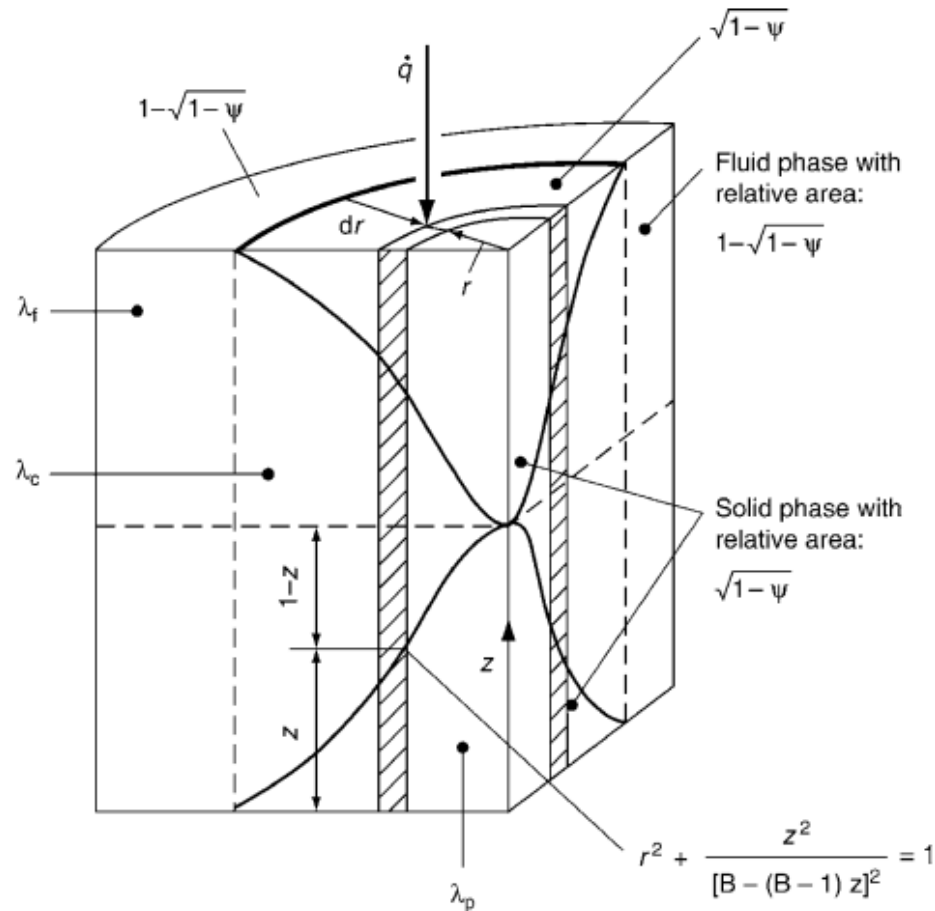
# Conclusion of research

- 1. New analytical calculation formula for the effective thermal conductivity coefficient for porous media with open pores has been proposed, which can be applied to the solar absorbers. The proposed formula includes dislocation vector that allows to calculate different porous structures with the same porosity value.
- 2. The proposed criterion dependence for the calculation of the Nusselt number includes the calculation of the lengths of the hydrodynamic and aerodynamic layers. The constants for the proposed dependencies for modern types of solar receiver absorbers are obtained. Validation of the results on a numerical model showed high reliability of the obtained results.



# Heat Transfer to Mechanically Agitated Beds with Latent Sink

**VDI Heat Atlas 2010:**



Unit cell of the model of Zehner/Bauer/Schlünder.

According to Fig. 3, the reduced thermal conductivity of the bed can be calculated to

$$k_{\text{bed}} = 1 - \sqrt{1 - \psi} + \sqrt{1 - \psi} k_c, \quad (5a)$$

with

$$k_c = \frac{2}{N} \left( \frac{B k_p - 1}{N^2 k_p} \ln \frac{k_p}{B} - \frac{B + 1}{2} - \frac{B - 1}{N} \right), \quad (5b)$$

and

$$N = 1 - (B/k_p), k_c = \lambda_c / \lambda_f. \quad (5c, d)$$

Here,  $\lambda_c$  is the thermal conductivity of the core of the unit cell [5]. The deformation parameter  $B$  is derived for spherical particles by putting the porosity of the unit cell equal to the porosity of the packed bed. This leads approximately to

$$B = 1.25 \left( \frac{1 - \psi}{\psi} \right)^{10/9}. \quad (5e)$$

Heat transfer kinetics can, again, be expressed in the form

$$\alpha_{\text{WS}} = \dot{q}_0 / (\vartheta_{\text{W}} - \vartheta_0), \quad (16)$$

$$\alpha_{\text{bed}} = \dot{q}_0 / (\vartheta_0 - \vartheta_{\text{bed}}). \quad (17)$$

The contact heat transfer coefficient  $\alpha_{\text{WS}}$  does not change in principle and can be calculated according to Sect. 4.1 for pure vapor atmosphere. On contrary, the consumption of heat by evaporation in the interior of the bed (the latent heat sink) has a significant influence on the penetration coefficient, which is in this case obtained to

$$\alpha_{\text{bed}} = \frac{2}{\sqrt{\pi}} \frac{\sqrt{(\rho \lambda c)_{\text{bed,dry}}}}{\sqrt{t_{\text{R}}}} \frac{1}{\text{erf } \zeta} = \frac{\alpha_{\text{bed,dry}}}{\text{erf } \zeta}. \quad (18)$$



# PRACTICAL SOLUTIONS IN DLR

Part 3 of „Heat and mass transfer in high temperature solar technology for cement production”



# Where are we?



Müller, Amelie und Harpprecht, Carina und Sacchi, Romain und Maes, Ben und van Sluisveld, Mariesse und Daioglou, Vassilis und Savija, Branko und Steubing, Bernhard (2024) [Decarbonizing the cement industry: Findings from coupling prospective life cycle assessment of clinker with integrated assessment model scenarios](#). Journal of Cleaner Production. Elsevier. doi: [10.1016/j.jclepro.2024.141884](#).

Overview of scenario results from IMAGE as input to LCA model			
	SSP2-Base (3.5°C)	SSP2-2.6 (2°C)	SSP2-1.9 (1.5°C)
<b>Foreground system</b>			
Process regionalization	26 IMAGE regions	26 IMAGE regions	26 IMAGE regions
Kiln technology mix	No CCS kilns	Mainly MEA CCS + DS CCS	Mainly MEA CCS + Oxy CCS
Fuel switch	Fuel shares stay largely similar	Higher uptake of modern biomass, large regional variations	Higher uptake of natural gas next to modern biomass, large regional variations
Clinker-to-cement ratio	71% CTC (global average) by 2060	67% CTC (global average) by 2060	65% CTC (global average) by 2060
Thermal energy efficiency <sup>a</sup>	Up to -13% by 2060, depend. on technology and region	Up to -21% by 2060, depend. on technology and region	Up to -21% by 2060, depend. on technology and region
Electric energy efficiency <sup>b</sup>	Up to -21% by 2060, depend. on technology	Up to -21% by 2060, depend. on technology	Up to -21% by 2060, depend. on technology
<b>Background system</b>			
Futurization of background system - electricity, steel, fuels, transport, CCS and non-CO <sub>2</sub> emission	IMAGE SSP2-Base	IMAGE SSP2-2.6	IMAGE SSP2-1.9

## 5. Conclusion

This study has presented a prospective life cycle assessment (pLCA) for the global clinker production until 2060 for a 3.5°C-baseline, 2°C- and 1.5°C-compatible scenario, using scenarios from the IMAGE integrated assessment model. A deep futurization of the supply chains in the life cycle inventory database ecoinvent v3.9.1 is achieved by combining scenarios for foreground clinker production with consistent scenarios for other major background sectors.

**Our life-cycle-based results show that a net-zero clinker production may not be achieved by 2060 with the production-oriented transition pathways considered in this study.** Using pLCA, any

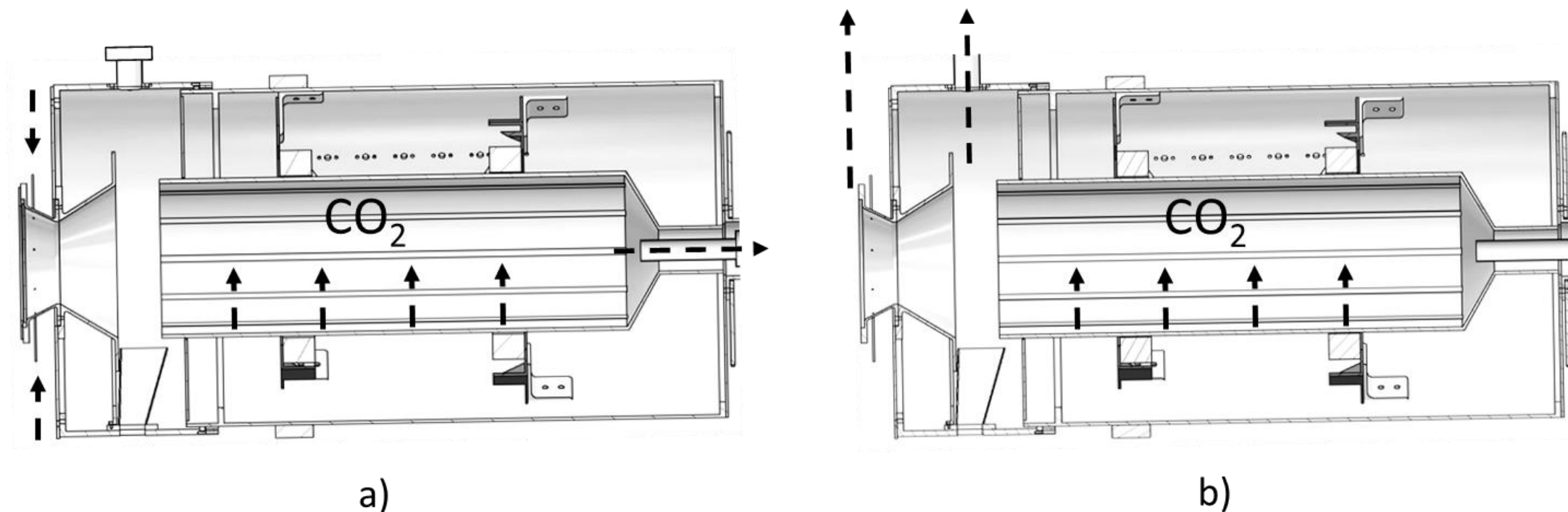
Fig. 3. Scenario results from IMAGE used in this study and their implications in the different scenarios. <sup>a</sup> Thermal energy efficiency from IMAGE undergoes corrections documented in Figs. A5–6, <sup>b</sup> electric energy efficiency is taken directly from IMAGE model documentation; see Table A9.

CCS - Carbon capture and storage

IMAGE - Integrated Model to Assess the Global Environment

CTC Clinker-to-cement

Visualisation of (a) the closed configuration where purge gas flow can be injected at the window and suction can be applied at the back and (b) the open configuration where suction can be applied before and behind the aperture

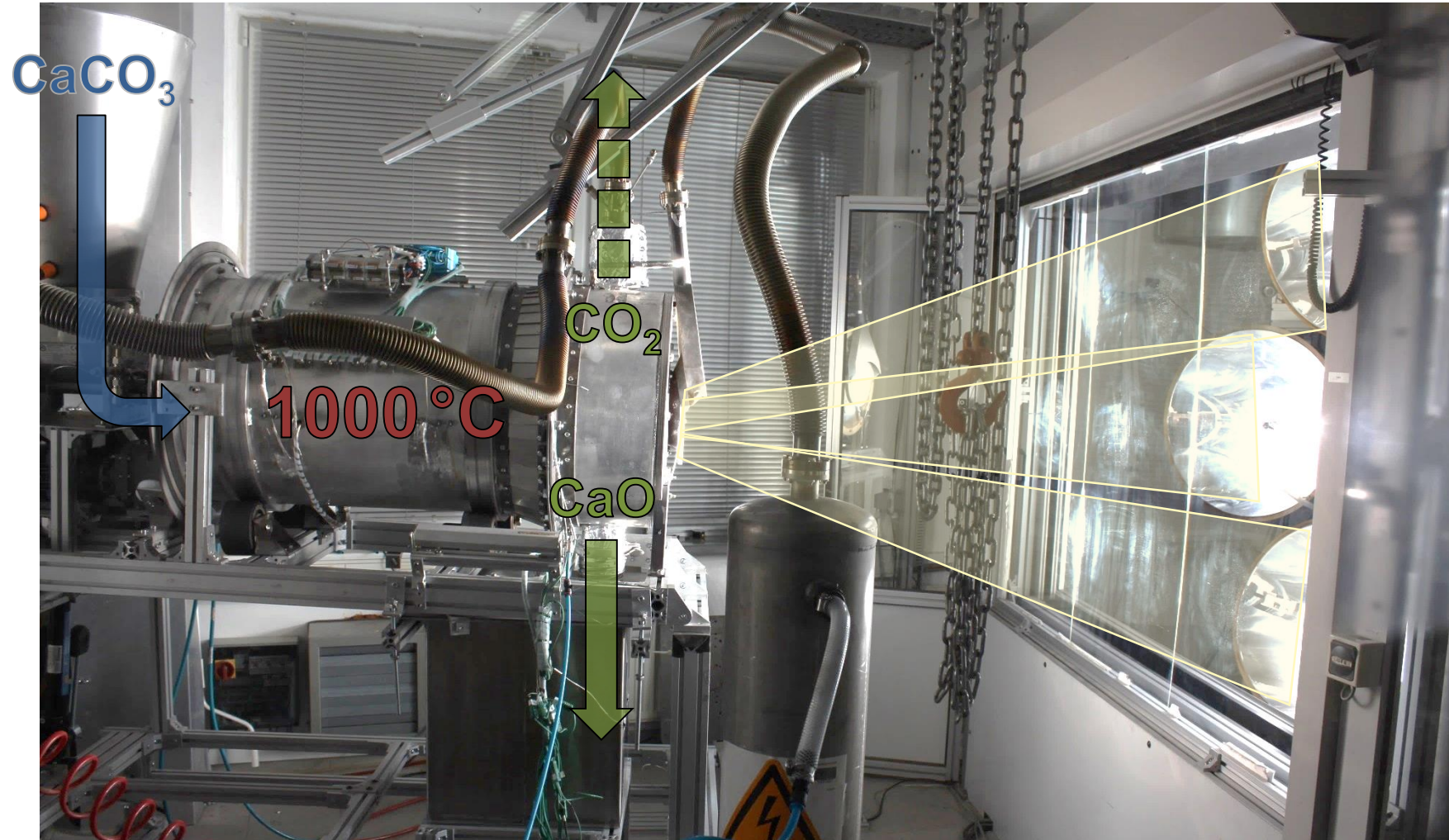


Source: Gkiokchan Moumin, Stefania Tescari et al. Solar treatment of cohesive particles in a directly irradiated rotary kiln. <https://doi.org/10.1016/j.solener.2019.01.093>.

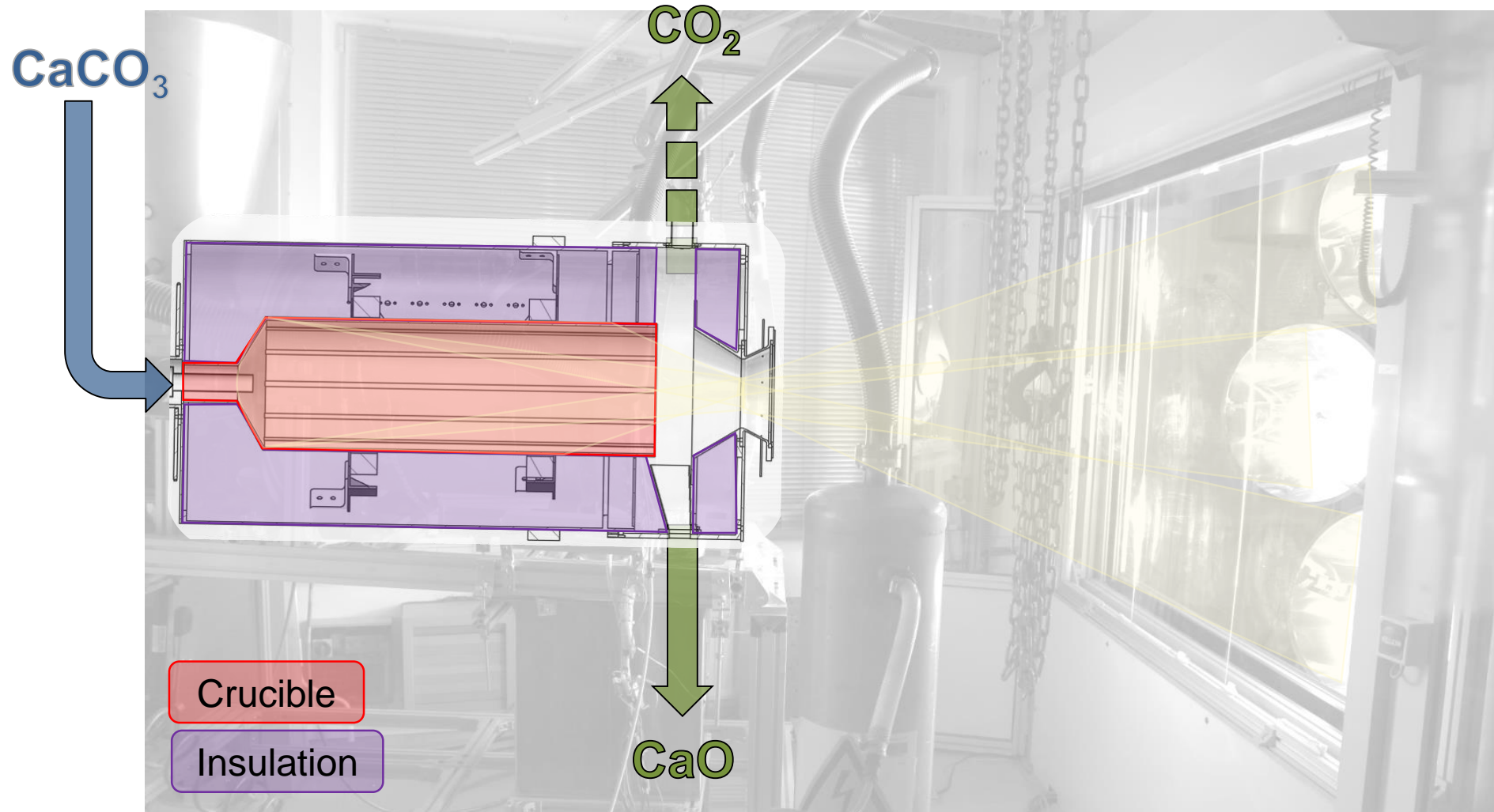


# Principle of solar rotary kiln for calcination

## Example: limestone



# Cut view of solar calciner





# Overview of research on the rotary kiln

## Completed

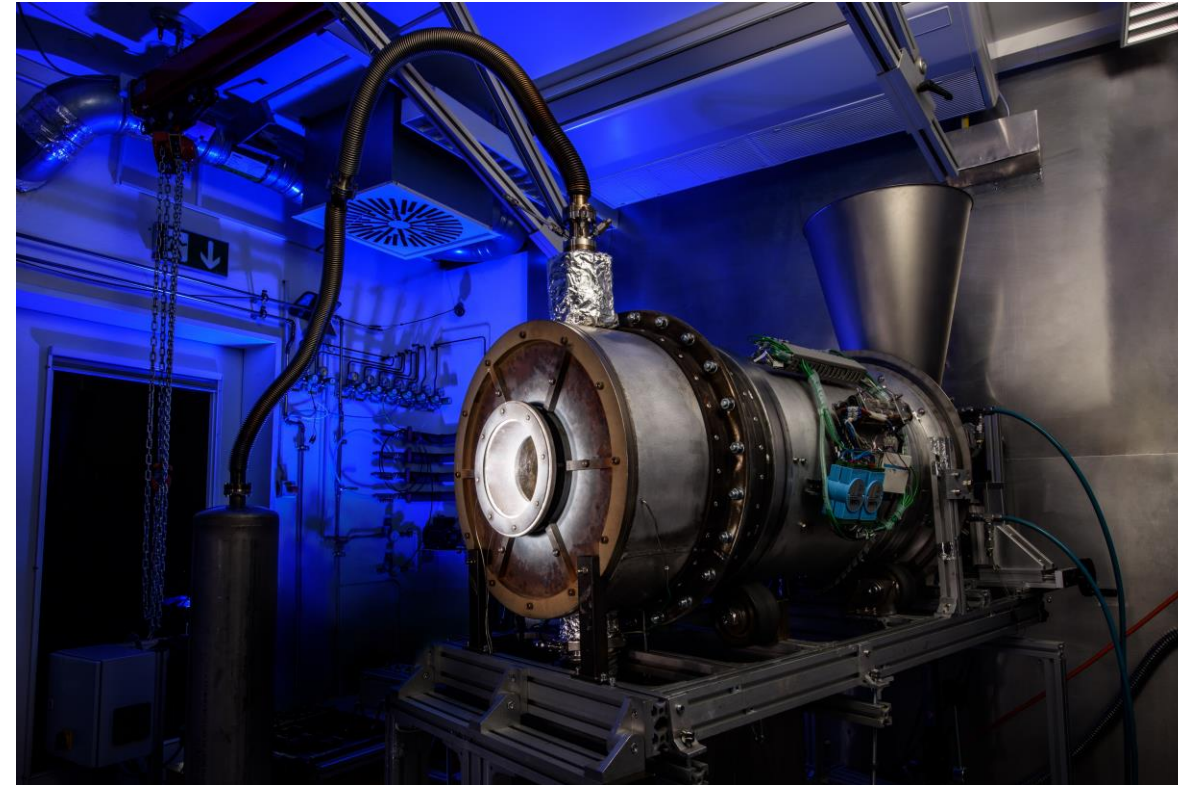
### Calcination of cement raw meal

- Industrial meal from the cement manufacturer
- 17 runs with calcination rates up to >95 %
- Treated continuous mass flow from 4-12 kg/h
- Heat input through radiation up to 14 kW
- Investigation of mixing and heat input

Openly accessible publications:

[Solar treatment of cohesive particles in a directly irradiated rotary kiln \(2019\)](#)

[Impact of bed motion on the wall-to-bed heat transfer for powders in a rotary kiln and effect of built-ins \(2021\)](#)





# Overview of research on the rotary kiln

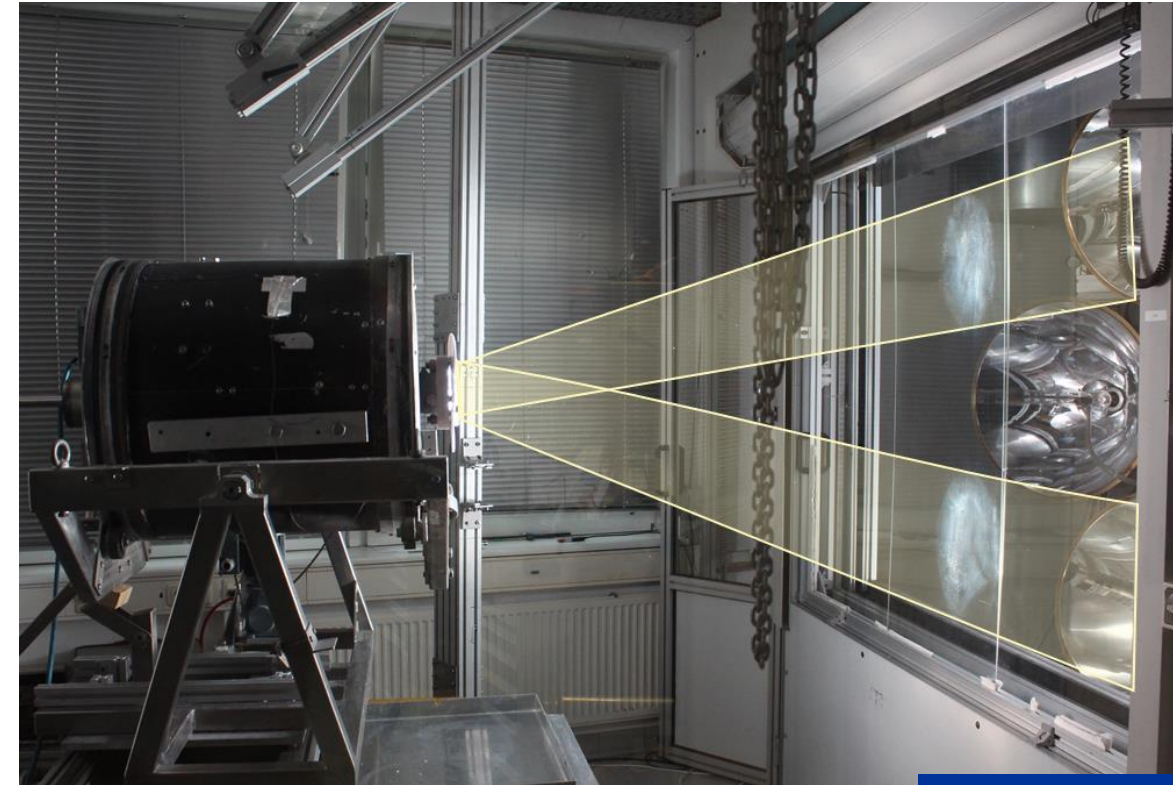
## Completed

### Calcination of kaolin and halloysite

- Raw materials from Turkey for the synthesis of zeolites (nanofilters)
- 20 runs in the temperature range 600-1000 °C
- Batch operation with 1 kg of material at a time
- Heat input through radiation up to 6 kW

Openly accessible publication:

[Solarization of the zeolite production: Calcination of kaolin as proof-of-concept \(2023\)](#)



# Overview of research on the rotary kiln

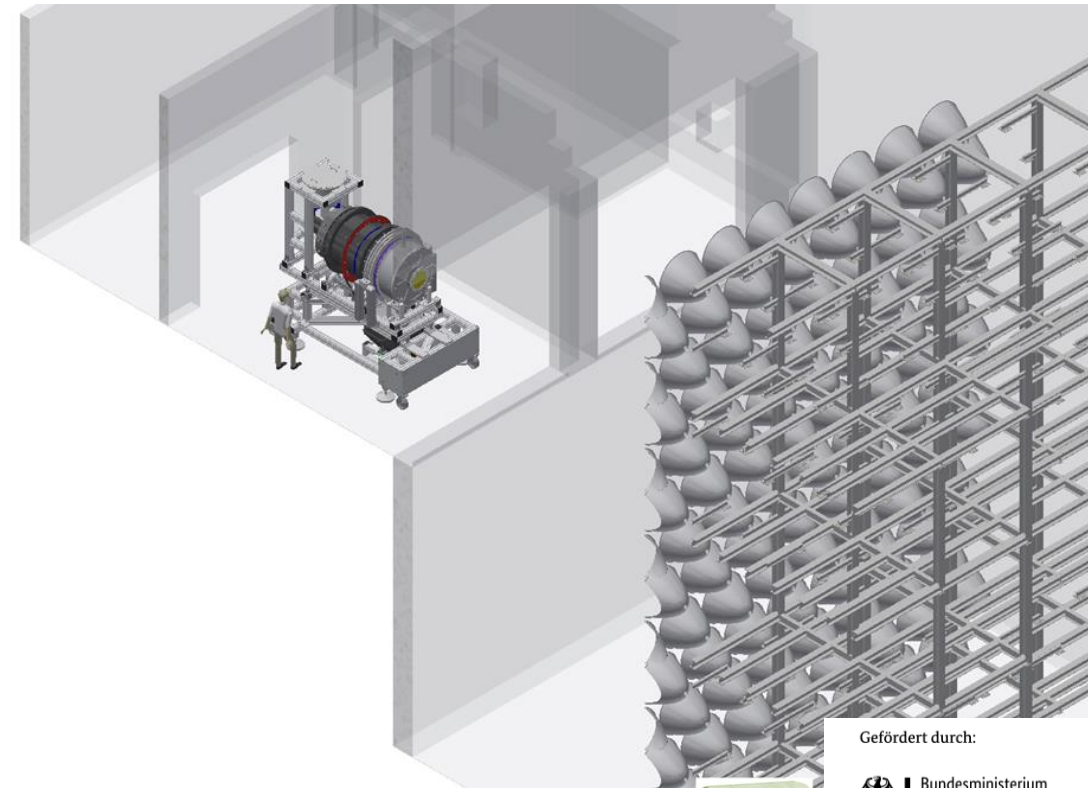
## Ongoing

### Calcination of limestone

- The aim is to feed quicklime into the cement process
- Continuous operation with 40-95 kg/h
- Heat input through radiation 50-100 kW
- As pure as possible separation of the CO<sub>2</sub>
- Trials planned for early 2025

Further information:

[BMWK project CemSol \(2021-2025\)](#)



Gefördert durch:



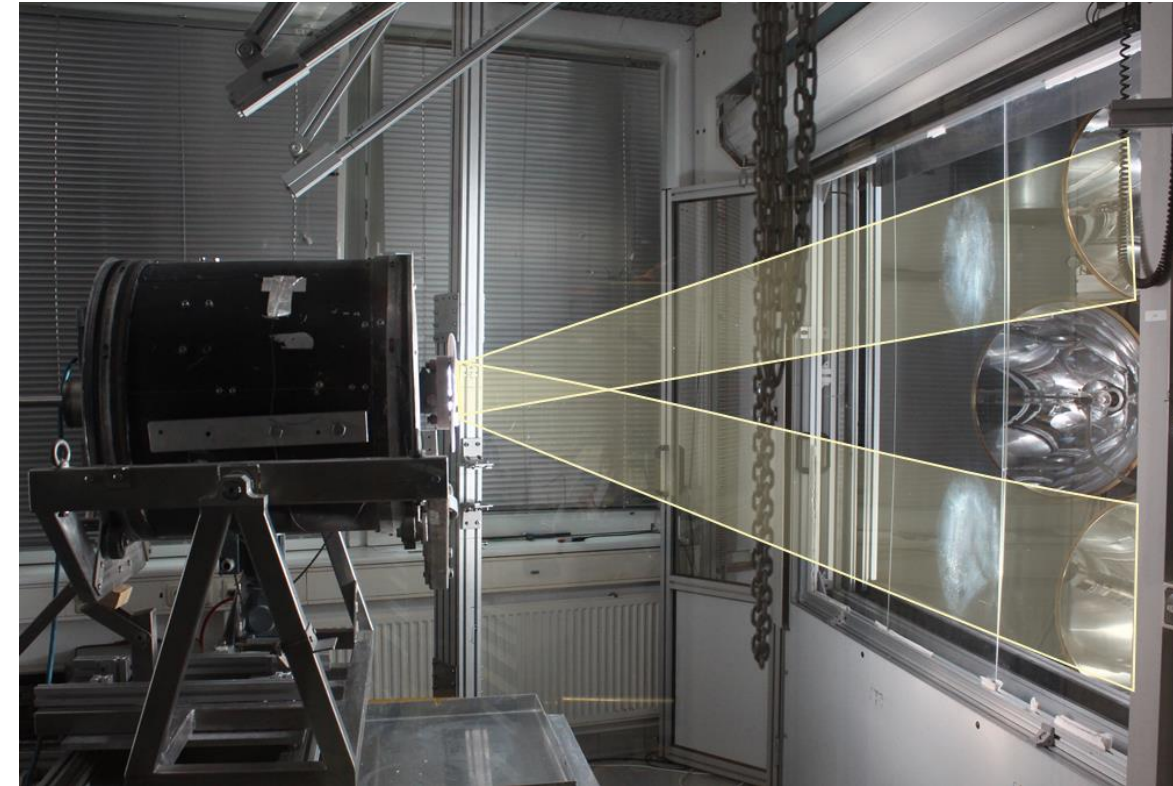
aufgrund eines Beschlusses  
des Deutschen Bundestages

# Overview of research on the rotary kiln

## Ongoing

### Calcination of kaolin

- Raw materials from Turkey for addition to cement as SCM
- Tests in the temperature range 600-1000 °C
- Batch operation with 1 kg of material at a time
- Heat input through radiation <10 kW





# Overview of research on the rotary kiln



In addition, studies and work in the field of

- Thermal treatment of dolomite
- Calcination and firing of magnesium carbonate
- Pyrolysis of biomass
- Reduction and oxidation of metal oxide particles

If you have any questions, please do not hesitate to contact me:

Dr.-Ing. **Gkiokchan Moumin** | Team Leader Carbon Management for Commodities

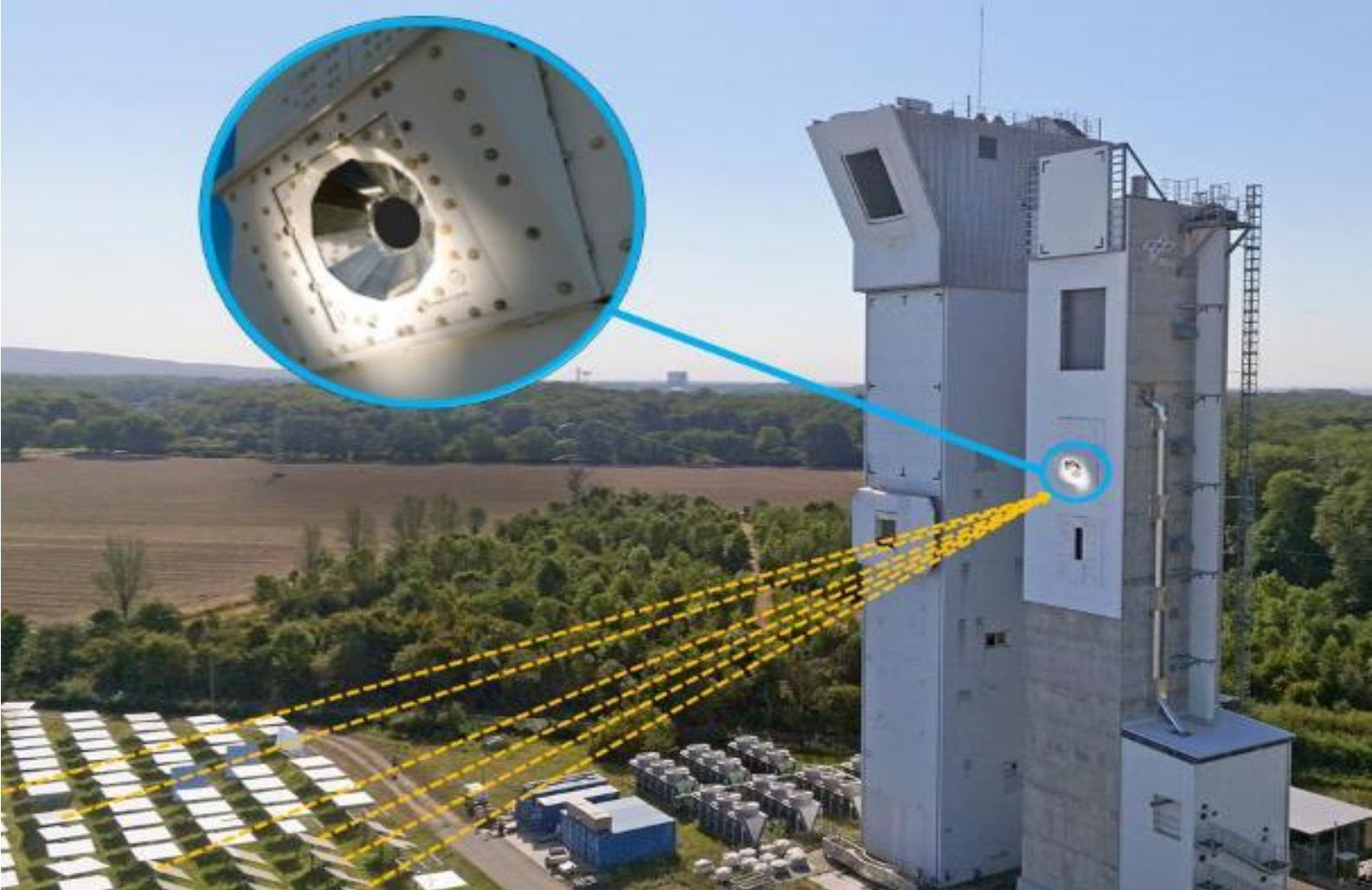
Phone +49 (0)2203 601-2353 | Fax +49 (0)2203 601-4170 | [gkiokchan.moumin@dlr.de](mailto:gkiokchan.moumin@dlr.de)

[DLR.de - Future Fuels](https://www.dlr.de/fuel)

**German Aerospace Center (DLR)**

Institute for Future Fuels | Solar-Chemical Process Development | Linder Höhe | 51147 Cologne

# Secondary concentrator



Source: DLR Stelleangebote

Cheilytko Andrii, DLR 26.11.2024 | New Delhy, Indian Institute of Technology Delhi

# Open Volumetric Air Receiver: Previous Design



## Volumetric Conical Receiver (VoCoRec):

- » Conical design – hexagonal cross-section
- » Ambient air is heated by flowing through a metallic wire mesh
- »  $T_{\text{air}} = 800 \text{ C}$
- » Calculated air return ratio ranges between 88 and 90%

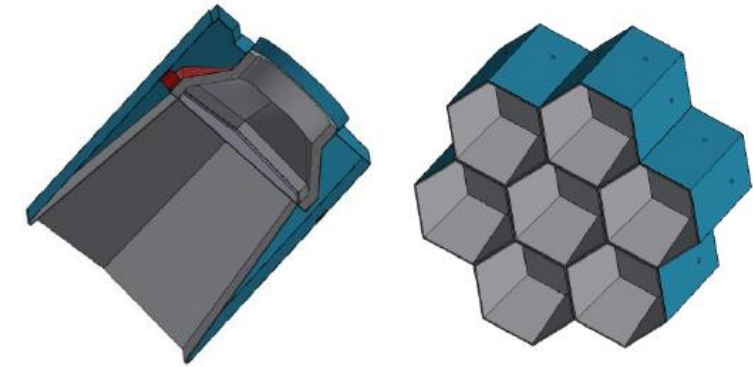
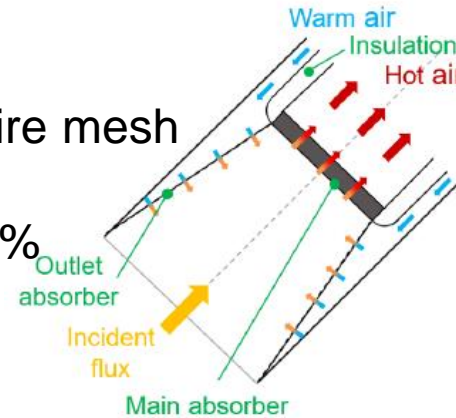
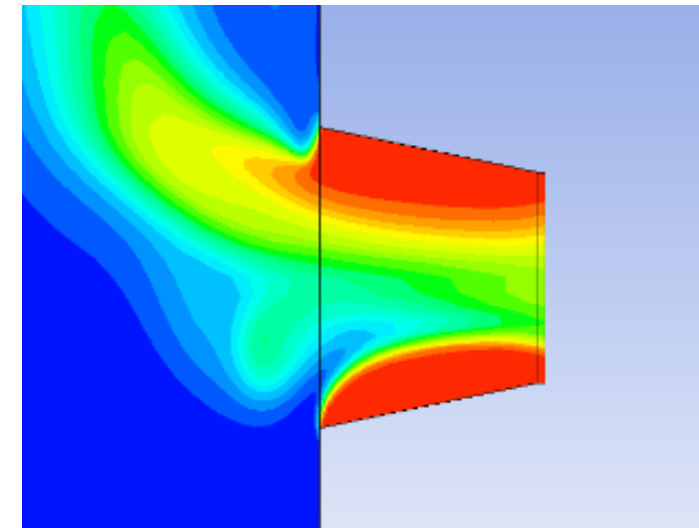


Illustration of VoCoRec

## Currently Research: attaining a higher Air Return Ratio (ARR) with an alternative configuration

### Alternative Design:

- » Conical design – Square cross-section
- » The inner section of the receiver is to be investigated using flow analysis
- »  $T_{\text{air}} \rightarrow 900 \text{ C}$





# Impressum



Thema: Heat and mass transfer in high temperature solar open volumetric receivers for cement production

Datum: 26.11.2024

Autor: Andrii Cheilytko: anrii.cheilytko@dlr.de

Institut: Institute for Solar Research, DLR

Bildcredits: Cheilytko A. Heat and mass transfer in high temperature solar open volumetric receivers for cement production. Work Shop. Department of Civil Engineering Indian Institute of Technology Delhi, New Delhi (26.11.2024)

For the first part, source is: Prof. Dr.-Ing. Robert Pitz-Paal. Institutspraesentation komprimiert: Solar research at the German Aerospace Center. 2023